
Article:
Jeddi, Neda, Scott, Neil W.J. and Fairlamb, Ian J.S. orcid.org/0000-0002-7555-2761 (2022) Well-Defined Pdn Clusters for Cross–Coupling and Hydrogenation Catalysis : New Opportunities for Catalyst Design. ACS Catalysis. 11615–11638. ISSN 2155-5435

https://doi.org/10.1021/acscatal.2c03345

ACS Catalysis

pubs.acs.org/acscatalysis

Review

Well-Defined Pd_n Clusters for Cross-Coupling and Hydrogenation Catalysis: New Opportunities for Catalyst Design

Neda Jeddi, Neil W. J. Scott, and Ian J. S. Fairlamb*

Cite This: *ACS Catal.* 2022, 12, 11615−11638

Read Online

ACCESS | Metrics & More | Article Recommendations

ABSTRACT: In recent studies it has been demonstrated that the privileged reactivity of higher-order metal clusters can be exploited in widely applied catalytic processes, particularly cross-coupling reactions and hydrogenative transformations. Relatively small, well-defined Pd_n clusters have been known since the 1960s. Unique reactivity, reaction (product) selectivity, and catalyst behavior have been recently uncovered, from which there is much potential in catalyst design and application. Ligated Pd_n clusters of a smaller size (where n is less than 6) may form upon degradation of mononuclear Pd species en route to larger particulate Pd (from <5 nm particles to large moribund forms in the >1 μm range). This review presents the catalytic applications of Pd_n clusters. We pay particular attention to the underlying structure of the Pd_n clusters, linked to their reactivity. A hypothesis that ligated Pd_n clusters may constitute a mechanism by which higher-order Pd species may form (as a bridging point for monoligated Pd species through to PdNPs) is further discussed. Where appropriate, we mention other catalytic reaction processes that complement the discussion focused on cross-coupling and hydrogenation processes.

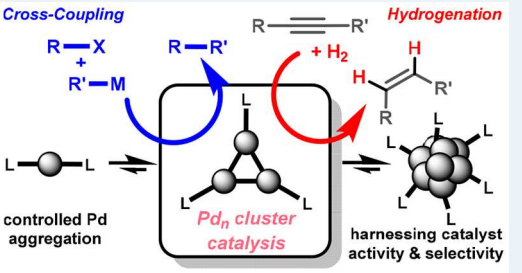

KEYWORDS: *palladium clusters, catalysis, cross-coupling, hydrogenation, catalyst speciation*

1. INTRODUCTION

Pd-catalyzed cross-coupling reactions constitute well-established methods for the formation of C−C and C−X (X = e.g. N, O) bonds, enabling access to an eclectic array of valuable organic materials.[1,2] Although tremendous efforts have been made to design mononuclear Pd complexes, which can boost the efficiency of catalytic processes, historically, less attention has been focused on the role of multinuclear cluster-type catalysts, either purposefully designed as distinct precatalysts or derived *in situ* under the reaction conditions.[3] Recently, researchers have examined the speciation of the Pd precatalysts while unraveling complex mechanistic pathways involved in the formation of catalytically active Pd_n clusters and small ligated species featuring Pd−Pd bonds in solution.[4−6] The conventional view is that cross-coupling catalysis is mediated either by low-coordinate Pd^0 monomeric species ($[Pd^0(L)_n]$, n = 1, 2) where $[Pd^0(L)_n]$ can be derived from pregenerated Pd^0 complexes such as $[Pd^0(PPh_3)_4]$ and $Pd_2(dba)_3$·X or by *in situ* reduction and activation of Pd(II) salt precursors such as $Pd(OAc)_2$ and $PdCl_2$,[7−9] enabled by two-electron-donor ligands (L), solvent, additives, or base.[10] Recent research nevertheless has supported the notion that higher-order Pd_n clusters are generated during the catalyst activation pathway, from preprepared complexes or from small-sized catalytically active heterogeneous PdNPs (<3 nm)[11] under certain reaction conditions which dominate catalytic processes involving reductive cross-couplings and hydrogenation reactions (Figure 1).[12−14] Other review articles have been compiled that discuss the synthesis and coordination chemistry of Pd clusters;[15,16] this review exclusively discusses Pd clusters in the context of catalysis, accompanied by relevant structural aspects which we believe are pertinent to productive catalysis.

Recent findings suggest that ligated dinuclear and trinuclear Pd species can form *in situ* using a mononuclear Pd^{II}/phosphine system with a specific ratio (stoichiometrically and catalytically).[17,18] Crucially, speciation events with given Pd^{II}/phosphine ratios that lead to the generation of higher-order Pd_n (n = 2, 3) species correlate well with differences in catalytic performance. These Pd_n species have been shown to act as catalytically competent species and demonstrate the ability to promote cross-coupling and hydrogenation reactions.[19−22] A complementary study by Corma[13,14] pointed toward ligand-free Pd_n clusters (n = 3, 4) derived from either Pd@EVOH (<5 nm) or Pd^{II} salts to be the catalytically active species under specific combinations of solvent and base in couplings (evidenced by UV−vis spectroscopy and DLS analysis). Such findings have shifted the traditional emphasis away from

Received: July 12, 2022
Revised: August 27, 2022

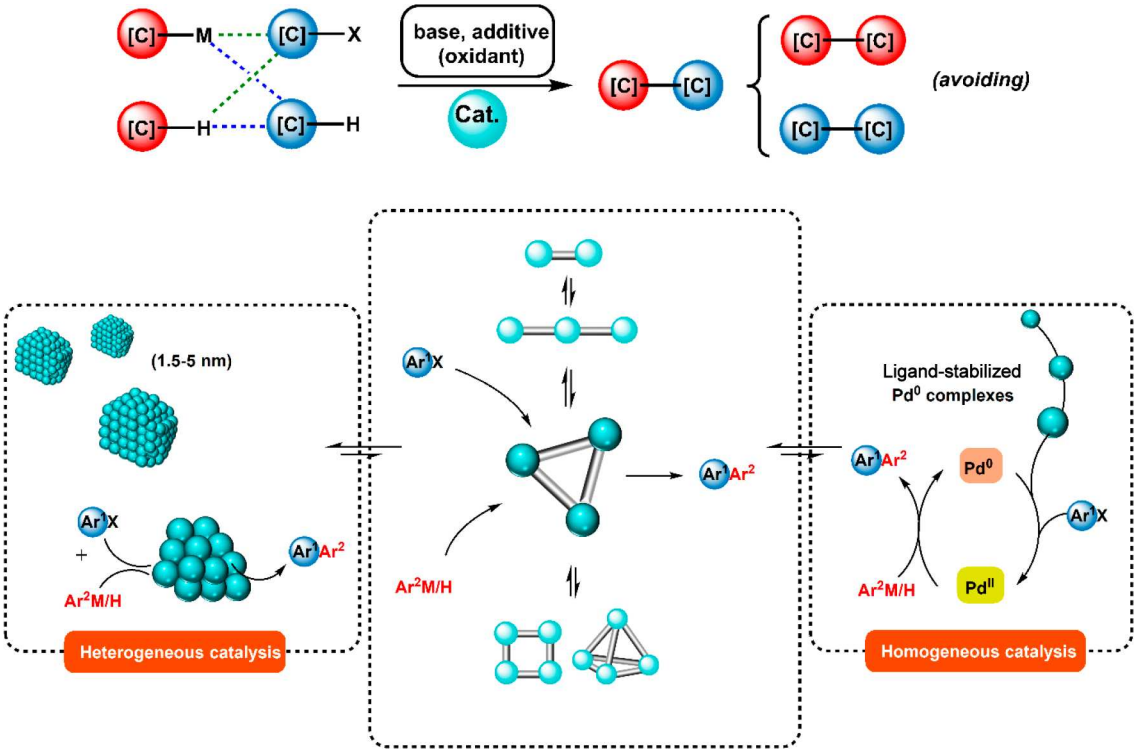

Figure 1. (top) Generalized cross-coupling processes bringing about the formation of carbon−carbon bonds. (bottom) Processes involved in generating high-nuclearity Pd clusters derived from either small nanoparticles or Pd^{II}/Pd^0 salts. Each of these higher-order species could be potentially stabilized by various components contained within the reaction medium.

exclusively evoking $[Pd^0(L)_n]$ as the accepted active species in cross-coupling reactions and have opened the door for well-defined, design of bespoke *in situ* generated Pd_n clusters, which can display reactive properties different from those of their monomeric counterparts.

While preformed high-nuclearity Pd_n clusters exhibit different kinetics and selectivity in cross-coupling reactions vs traditional mononuclear $[Pd^0(L)_n]$ species,[19,23] the speciation of the catalysts that result *in situ* from the formation of clusters with different activities could, *inter alia*, address an issue in the process of developing a catalytic system. However, exploring the differences between the reactivities of different types of Pd clusters, formed under working reaction conditions, could provide an opportunity to augment either preformed higher-order palladium complexes or to find optimal conditions to generate a desired Pd_n cluster species *in situ*. One can expect that the reactivity and selectivity of the catalyst could be modulated in different transformations. Furthermore, an investigation of the mechanism behind the catalyst propagation, speciation, and catalytic roles of these species could leverage opportunities that aid improvement of resource efficiency and reaction atom economy in industrial processes. These topics are explored in detail within this review. Where appropriate, we mention other catalytic reaction processes that complement the discussion focused on cross-coupling and hydrogenation processes.

2. CATALYTIC ACTIVITY OF PD_N SPECIES

2.1. Formation of Pd Clusters from Pd^I Dinuclear Complexes. The simplest type of Pd−Pd-bonded systems are dinuclear complexes. Recently, a wealth of powerful and diverse applications of dinuclear Pd^I complexes have been reported and shown, in several cases, to act as a precursor to higher nuclearity systems. An early example of a catalytic cross-coupling application of a Pd^I dinuclear complex was reported in 2002 using $[Pd(\mu\text{-Br})(P\text{-}t\text{-}Bu_3)]_2$,[24−26] which was identified as a highly active catalyst for challenging-to-activate aryl chloride bonds for amination reactions (which we commonly now refer to as Buchwald−Hartwig reactions)—the cutting edge for cross-coupling catalyst efficacy at the time (Scheme 1).[27]

Scheme 1. Buchwald−Hartwig Amination of Aryl Chlorides with $[Pd_2Br_2(PR_3)_2]$ under the Optimized Reaction Conditions

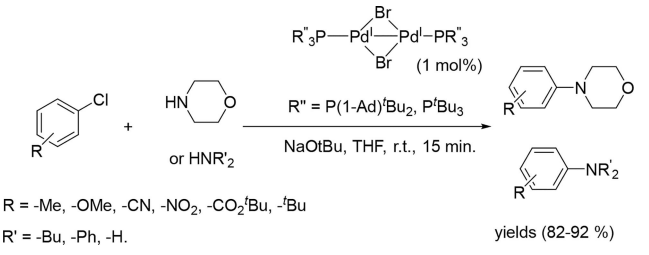

Such Pd^I dinuclear complexes, adopting the formula $[Pd^I(\mu\text{-}X)(PR_3)]$ (where PR_3 is a tertiary organophosphine; X = Br, I), have been shown to activate by disproportionation and release of monoligated Pd^0 species.[28,29] In other cases, they have been shown to enable transformations as intact dinuclear Pd complexes.[30] The details concerning the mechanism of reactivity of Pd^I dimers is beyond the scope of this review, and we point readers to another excellent minireview.[6] Examples, however, of such dinuclear Pd complexes acting as precursors for catalytically active higher nuclearity species, including

https://doi.org/10.1021/acscatal.2c03345
ACS Catal. 2022, 12, 11615−11638

Scheme 2. Synthesis of a Pd_3 Trimer Cluster from Dimeric $[Pd(\mu\text{-}Br)(P^tBu_3)]_2$, Following the Stoichiometric Reactivity with *p*-Iodoacetophenone (Top) and Chemoselective Arylation Using the Trinuclear Pd Complex as a Catalyst (Bottom)

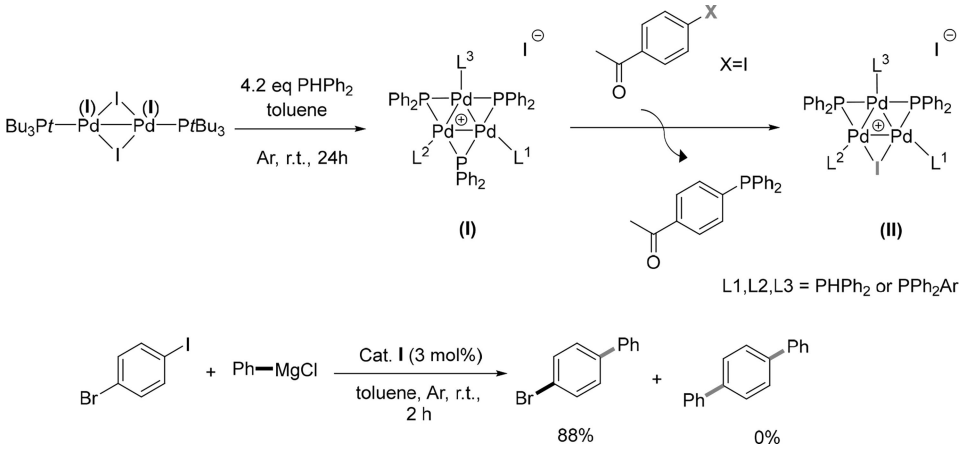

Scheme 3. Reductive Disproportionation of the Isocyanide-Stabilized Pd^I Dimer III Forming the $Pd^0{}_3$ Cluster Complex IV

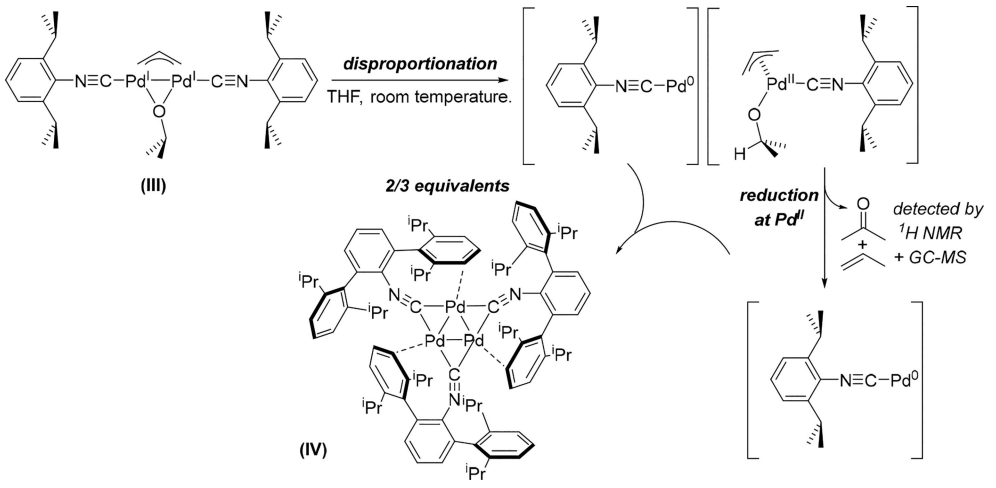

clusters, have recently come to light and will be discussed below.

Treatment of the iodide-bridged Pd^I–Pd^I dimer $[Pd^I(\mu\text{-}I)(P\text{-}t\text{-}Bu_3)]_2$ species with an excess of the secondary phosphine diphenylphosphine led to the quantitative formation of the cationic trimeric Pd cluster $[Pd_3(\mu\text{-}PPh_2)_3(PHPh_2)_3]^+$ (**I**) (Scheme 2).[23] This Pd cluster reacted with stoichiometric 4-iodoacetophenone to form $[Pd_3(\mu\text{-}I)(\mu\text{-}PPh)_2(PHPh_2)_3]^+I^-$ (**II**), with concomitant formation of a new tertiary phosphine that remained in dynamic exchange with the cluster. The Pd trimer proved to be catalytically competent, although the fate of the P-*t*-Bu_3 ligand was not reported. Conversion on exposure to 4-iodoacetophenone points toward a different, albeit related, tripalladium species being present after the first catalytic turnover, under relevant cross-coupling conditions.

The phosphido-bridged trimer showed a high chemoselectivity for C(sp^2)–I bonds over C(sp^2)–Br and C(sp^2)–Cl bonds in Kumada cross-couplings (as expected based on bond dissociation energies of the C–X bonds) (Scheme 2).[31] Such high chemoselectivity observed with **I** was not obtained with either its precursor $[Pd^I(\mu\text{-}I)(P\text{-}t\text{-}Bu_3)]_2$ or commonly employed mononuclear Pd^{II} and Pd^0 catalyst precursors. Ultimately, converting the Pd^I complex to a Pd_3 complex resulted in more controlled reactivity—effectively the reactivity was tempered such that the trimer activates C–I more selectively than other halides.

In 2017, when they investigated the role of bulky, π-accepting isocyanide-containing ligands ($CNAr^{Dipp2}$)[32] in Pd cross-coupling catalysis, Figueroa et al. discovered that the Pd^0 cluster $[Pd^0{}_3(\eta^2\text{-Dipp-}\mu\text{-}CNAr^{Dipp2})_3]$ (**IV**) (Scheme 3)[33] formed after the spontaneous reductive disproportionation of an allyl- and alkoxide-bridged Pd^I dinuclear complex at room temperature $[(\mu\text{-}C_3H_5)(\mu\text{-}X)Pd^I(CNArDipp_2)]_2$ (**III**), eliminating acetone and propene as oxidized side products. Each Pd atom in the product cluster hence exhibited a formal oxidation state of zero—in essence making it a trimer of three monoligated $[Pd^0(CNArDipp_2)_1]$ complexes, stabilized by bridging, π-accepting isocyanide ligands in addition to η^2-C,C interactions from the Pd centers (Pd–Pd bond distance 2.6353(5)). The cluster species **IV** was found to be competent as a catalyst in room-temperature SMCC reactions of aryl bromides at room temperature, outperforming the Pd^I dinuclear precursor complex **III** under the same conditions, but performed slightly poorer than the independently synthesized monomeric bis-ligated Pd^0 complex $[Pd^0(CNArDipp_2)]_2$.

The above study shows that an unstable, reactive Pd^I dinuclear complex can convert to a stabilized Pd_3 cluster, demonstrating that low-ligated Pd may be stabilized by

https://doi.org/10.1021/acscatal.2c03345
ACS Catal. 2022, 12, 11615–11638

aggregation to well-defined ligated clusters. In this case it is likely that further aggregation, which may have otherwise occurred with analogous unprotected electron-rich Pd complexes, was prevented by the bulky and π-electron-accepting quality of the coordinated isocyanide ligand. An example in which an isocyanide-ligated Pd_3 cluster is converted to another, catalytically active Pd_3 cluster is discussed in the next section.

While the preceding examples have shown that Pd monomers and dimers can be converted into trimers with relevance to catalytic processes, there is precedent for the reverse being possible. In 1987, Jones et al. discovered that the CO-ligated tripalladium cluster $[Pd_3(\mu\text{-P-}t\text{-Bu}_2)_2(\kappa\text{-CO})_2(\kappa\text{-Cl})]$, bridged by *tert*-butylphosphido groups, could fragment and the CO ligands be fully substituted after treatment with σ-electron-donating PMe_3 to form the phosphido-bridged Pd^I dimeric species $[Pd^I(\mu\text{-P-}t\text{-Bu}_2)(PMe_3)]_2$.[34]

In a ground-breaking series of studies in the early to mid 1990s, Amatore and Jutand et al. demonstrated that, when it was treated with excesses of simple PPh_3, $Pd(OAc)_2$ was ultimately reduced to the Pd^0 complexes $[Pd^0(PPh_3)_n]$ (in exchange with $^-$OAc anion in solution).[7,35−37] This phenomenon was shown to proceed via an intramolecular reduction at Pd^{II} by a sacrificial 1 equiv of PPh_3, which was concomitantly oxidized to O═PPh_3. Fairlamb et al. subsequently showed that quite different speciation events occur when $Pd(OAc)_2$ reacts at room temperature in the presence of 2 or 1 equiv of PPh_3 per Pd atom. When $Pd(OAc)_2$ reacts directly with 1 equiv of PPh_3, Pd particles ultimately form.[38] Treating $Pd(OAc)_2$ with 2 equiv of PPh_3, however, resulted in the formation of the phosphido- and acetato-bridged Pd^I dinuclear complex $[Pd_2(\mu\text{-OAc})(\mu\text{-PPh}_2)(PPh_3)_2]$ (**V**) (Scheme 4).[17] The more

Scheme 4. Known Speciation Events Leading to the Formation of $[Pd(\mu\text{-X})(\mu\text{-PPh}_2)_2(PPh_3)_3]^+Y^-$ Clusters from $Pd(OAc)_2$ and 2 equiv of PPh_3

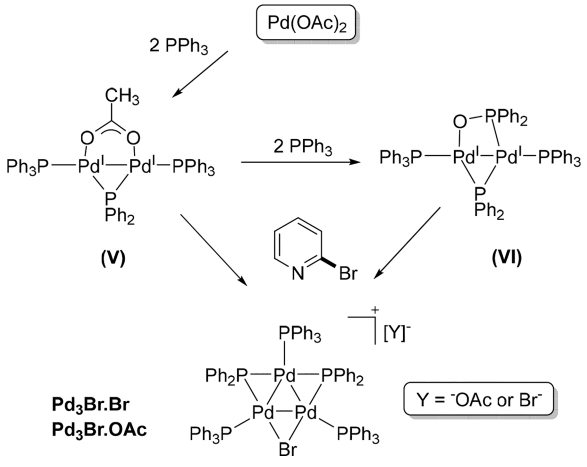

electron-rich phosphine dialkylbiaryl (Buchwald) ligands (e.g., XPhos and SPhos) have been shown to similarly form phosphido-stabilized Pd^I dinuclear complexes, on *in situ* reduction of $Pd(OAc)_2$.[39] Bedford and co-workers characterized Pd^I dinuclear complexes bearing strong analogy with **V**; in both cases, a stabilizing phosphido group was proposed to form by Pd-mediated P−C bond scission.[40] On reaction with further PPh_3 (2 equiv), the complex **V** was shown to disproportionate, forming a new phosphido- and κ_2-*P,O*-μ-phosphinito-bridged Pd^I dimer, alongside the mononuclear complex $[Pd^0(PPh_3)_3]$ and acetic anhydride.[41] A κ_2-*O,O*-μ-phosphinato- and phosphido-bridged dimer was also isolated in the solid state from the reaction mixture; however, it was not observed spectroscopically.

Crucially, upon reaction with organohalides such as 2-bromopyridine, the dinuclear complex $[Pd_2(\mu\text{-OAc})(\mu\text{-PPh}_2)(PPh_3)_2]$ was shown to form cationic tripalladium clusters of the type $[Pd(\mu\text{-X})(\mu\text{-PPh}_2)_2(PPh_3)_3]^+Y^-$ (Scheme 4; X = halide; Y = halide, acetate), carrying an average oxidation state of 4/3 per Pd. The dimeric $[Pd(Br)(N\text{-}C^2\text{-pyridyl})(PPh_3)]_2$ complex formed as a byproduct. Similarly, when the phosphinito-bridged Pd^I dinuclear complex $[Pd_2(\mu\text{-PPh}_2)(\kappa_2\text{-}P,O\text{-}\mu\text{-P(O)Ph}_2)(\kappa\text{-PPh}_3)_2]$ (**VI**) reacted with 2-bromopyridine, $[Pd(\mu\text{-Br})(\mu\text{-PPh}_2)_2(PPh_3)_3]^+Y^-$ was formed (Scheme 4).

The ratio of 1 equiv of $Pd(OAc)_2$ to 2 equiv of PPh_3 was crucial for formation of the Pd_3 cluster species, which also led to marked changes in catalyst activity, as compared to that when higher (≥3 equiv) amounts of PPh_3 were used. For example, the kinetic profile for a model Suzuki−Miyaura cross-coupling (SMCC) reaction of 2-bromopyridine with *p*-fluorophenylboronic acid catalyzed by $[Pd_3(OAc)_6]$/6PPh_3 (Pd:PPh_3 = 1:2) (Scheme 5) as well as preformed $[Pd(\mu\text{-Br})(\mu\text{-PPh}_2)_2(PPh_3)_3]^+Br^-$ and its precursor **V** showed comparable, relatively fast reaction efficacies and conversions. On the other hand, when $Pd(OAc)_2$/≥3 equiv of PPh_3 or $[Pd^0(PPh_3)_3]$ was employed as the catalyst under otherwise the same conditions, sluggish kinetics were observed and a higher reaction temperature of 70 °C was required to induce good product conversion.

Scheme 5. Model SMCC Conditions Used for Performance Comparison of $Pd(OAc)_2$ and *n* equiv of PPh_3, vs Preformed Mononuclear and Multinuclear Complexes

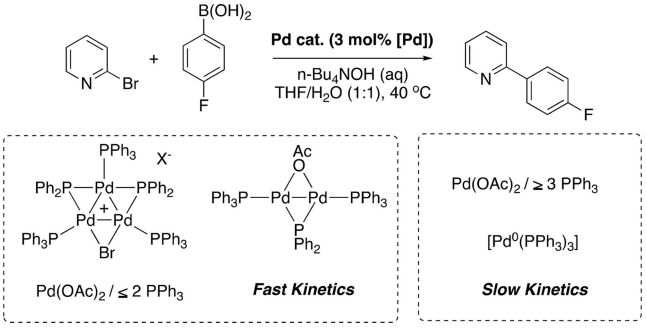

Under SMCC reaction conditions similar to those above, but with the dihalogenated heterocyclic substrate 2,4-dibromopyridine in place of 2-bromopyridine, site-selectivity differences were observed as a function of the catalyst system used (Scheme 6). $Pd(OAc)_2$/≥3 PPh_3, $[Pd^0{}_2(dba)_3{\cdot}CHCl_3]$/2$PPh_3$, and $[Pd^0(PPh_3)_4]$, systems known to generate mononuclear $[Pd^0(PPh_3)_n]$-type species,[42,43] mediated coupling at the typical C2 site, in line with previous findings by Cid et al. using the mononuclear precatalyst $[Pd^0(PPh_3)_4]$.[44] However, $[Pd(\mu\text{-Cl})(\mu\text{-PPh}_2)_2(PPh_3)_3]^+Cl^-$, $[Pd_2(\mu\text{-OAc})(\mu\text{-PPh}_2)(PPh_3)_2]$, or $Pd(OAc)_2$ with 1 or 2 equiv of PPh_3—ratios known to form clusters under stoichiometric conditions—showed selectivity for the atypical C4 site of 2,4-dibromopyridine.

A crucial role for additive salts was delineated under both Suzuki−Miyaura and Kumada−Corriu cross-coupling con-

https://doi.org/10.1021/acscatal.2c03345
ACS Catal. 2022, 12, 11615−11638

Scheme 6. Model Suzuki–Miyaura Conditions Used for Assessing the Site Selectivity of $Pd(OAc)_2$ and *n* equiv of PPh_3, vs Preformed Mononuclear and Multinuclear Complexes at the Dihalogenated Substrate 2,4-Dibromopyridine

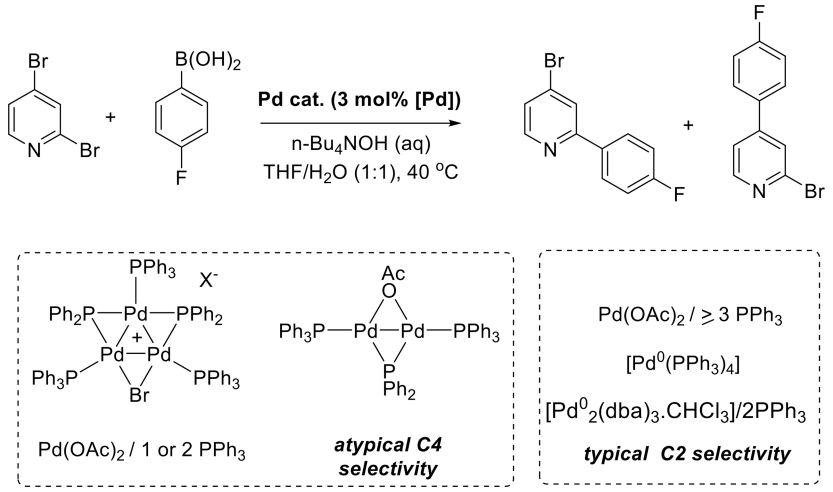

ditions, indicating likely conversion to an active PdNP species under catalytic conditions, in line with previous literature precedents.[45,46] Taken together, this work showed that, when information regarding catalyst speciation is known, this information can be exploited to tune catalyst activity.

The above recent investigations found the catalytic competence of higher-order Pd species generated when high $Pd:PR_3$ ratios were employed, as well as their higher reactivity than traditional mononuclear Pd^0 complexes generated *in situ* from a low $Pd:PR_3$ ratio. Hence, exploring the role of Pd_n clusters in catalysis processes and understanding the mechanism behind the reduction of Pd species would be of high importance in the area of catalyst design and control of *in situ* catalyst speciation. Formation of $[Pd_2(\mu\text{-OAc})(\mu\text{-PPh}_2)(PPh_3)_2]$ from simple mononuclear Pd^{II} precursor complexes, which are able to go on to form Pd_3 clusters, highlights how one can access new catalyst manifolds with potentially unique reactivity.

2.2. Well-Defined Clusters as Catalysts. The above examples have shown that Pd clusters may form from mononuclear and interconvert from dinuclear sources, under stoichiometric conditions, with crucial relevance to cross-coupling catalysis. In several examples, clusters of the form $[Pd(\mu\text{-X})(\mu\text{-PPh}_2)_2(PR_3)_3]^+Y^-$ (X = Cl, Br, I; Y = halide, SbF_6, OAc, BF_4) ($Pd_3X{\cdot}Y$) were seen to form under (pseudo)-catalytic conditions. This structural motif has been studied quite extensively over the years (Scheme 7). Several derivatives have been characterized. As early as 1968, Coulson et al. found that the direct reaction between $PdCl_2$ and $[Pd^0(PPh_3)_4]$ resulted in the formation of the tripalladium cluster $[Pd_3(\mu\text{-Cl})(\mu\text{-PPh}_2)_2(PPh_3)_3]^+Cl^-$ alongside *trans*-$[PdCl(Ph)(PPh_3)_2]$, which was formed as a byproduct of the cleavage of PPh_3.[47] It was hypothesized that in this synthesis $PdCl_2$ acted to scavenge PPh_3, affording a highly reactive, low-coordinate $[Pd^0(PPh_3)_n]$ which initiated the observed clustering.

Dixon et al. later reported the precise structure of the related $[Pd_3(\mu\text{-Cl})(\mu\text{-PPh}_2)_2(PPh_3)_3]^+[BF_4]^-$ and some of its derivatives, by use of ^{31}P NMR spectroscopic and X-ray diffraction analysis after devising a new synthesis by decomposition of $[PdCl(PPh_3)_2]^+[BF_4]^-$ in supercritical THF.[48,49] The structure was found to be planar with respect to the three Pd and five P atoms. Three Pd atoms formed an approximately equilateral

Scheme 7. Different Ways That Tripalladium Clusters of the Type $[Pd_3(\mu\text{-X})(\mu\text{-PPh}_2)_2(PPh_3)_3]^+Y^-$ Can Be Synthesized by Reduction of Pd^{II} Salts

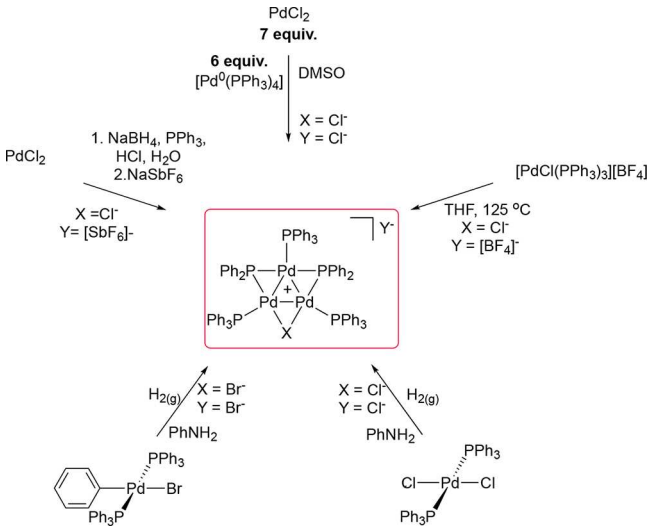

triangle, stabilized by two bridging diphenylphosphido ligands and one bridging chloride ligand, each capped with a PPh_3, two $\mu\text{-PPh}_2$ anionic bridges and one μ-Cl anionic bridge, giving a formal oxidation state of 4/3 per Pd. Moiseev et al. subsequently found that hydrogenation of $[PdCl_2(PPh_3)_2]$, $[PdCl_2(PPh_3)]_2$, or $[PdBr(Ph)(PPh_3)_2]$ with molecular hydrogen in the presence of an organic amine solvent resulted in the formation of $[Pd_3(\mu\text{-X})(\mu\text{-PPh}_2)_2(PPh_3)_3]^+X^-$ (X = Cl, Br, varying depending on the parent complex).[50] The same group similarly discovered that $[Pd_3(OAc)_6]$ salts could be hydrogenated to form a variety of different Pd clusters, the structures of some of which have not yet been fully elucidated.[51] These syntheses show that higher-order Pd cluster structures readily form as stable species under reducing (hydrogenic) conditions, from simple Pd precursor complexes.[52]

Li et al. reported the first catalytic application of Coulson's $[Pd_3(\mu\text{-Cl})(\mu\text{-PPh}_2)_2(PPh_3)_3]^+[SbF_6]^-$ cluster structural motif, examining its performance in SMCC reactions.[19] When it was applied as a precatalyst, $Pd_3Cl{\cdot}SbF_6$ demonstrated high activity at very low catalyst loadings (0.08 mol %) in the

https://doi.org/10.1021/acscatal.2c03345
ACS Catal. 2022, 12, 11615–11638

Scheme 8. Pd_3-Catalyzed SMCC Reaction Using 0.08 mol % $Pd_3Cl{\cdot}SbF_6$ Catalyst Loading under Optimized Reaction Conditions (Top) and Single-Crystal X-ray Structure of the $Pd_3Cl{\cdot}SbF_6$ Catalyst (Bottom)[a]

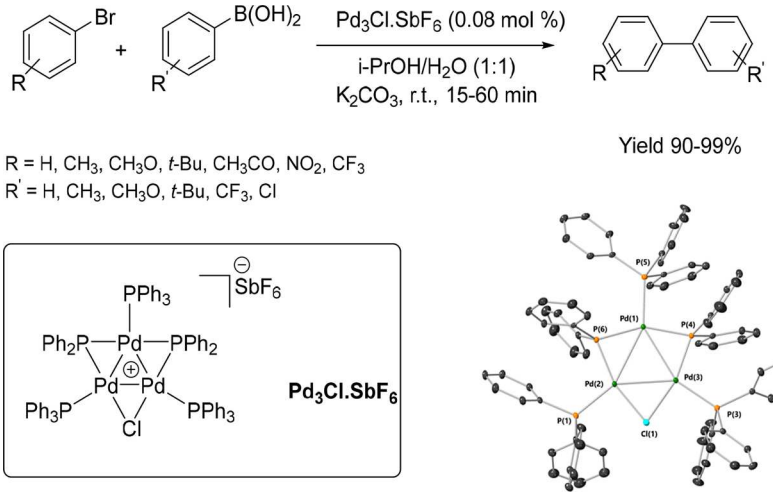

[a]The crystal structure of the catalyst was reprocessed in CrystalMaker X. Thermal ellipsoids are shown at the 20% probability level. The SbF_6 anion and hydrogen atoms are removed for clarity.

formation of a variety of *para*-substituted biaryls (Scheme 8). The $Pd_3Cl{\cdot}SbF_6$ cluster was shown to be robust on exposure to air and found to be stable up to 170 °C in the solid state.[19]

Based on the results provided by NMR spectroscopic experiments, UV−vis, ESI-MS, and EXAFS analysis, it was reported that the $Pd_3Cl{\cdot}X$ cluster remains intact during the catalytic reaction, under the conditions, with the μ-Cl ligand exchanging for a μ-Br during reaction progression. Stoichiometric reactions were employed to gain insight into the catalyst's mechanism of action. The reagents were individually reacted with the cluster under the reaction conditions derived from those in the catalytic SMCC reaction. ESI-MS and EXAFS experiments both indicated the formation of the new species $[Pd_3(\mu\text{-Ar})(\mu\text{-PPh}_2)_2(PPh_3)_3]^+$ (Pd_3Ar^+) by treating the Pd_3Cl^+ cluster with phenylboronic acid in the presence of K_2CO_3 in dichloromethane. On the other hand, the reaction of the cluster with phenyl bromide under like conditions, in the presence of K_2CO_3, did not lead to the formation of Pd_3Ar^+ as analyzed by ESI-mass spectrometry. Additionally, under these conditions, in the absence of either bromobenzene or phenylboronic acid substrate, the presence of an ion corresponding to the mass of $[Pd_3(\mu\text{-OH})(\mu\text{-PPh}_2)_2(PPh_3)_3]^+$ (Pd_3OH^+) was detected (MALDI-MS), along with other uncharacterized species. Based on these data, it was concluded that, under SMCC conditions, a Pd_3Cl^+ catalyst initially reacts with *in situ* generated hydroxide (presumably at low concentration), which subsequently reacts with phenylboronic acid to generate a Pd_3Ar^+ intermediate. In the following step, the Pd_3Ar^+ intermediate was hypothesized to react with bromobenzene in a σ-bond metathesis process, resulting in biaryl product formation and leading to the regeneration of the catalytic species (as Pd_3Br^+) (Figure 2).

Such a postulated reactivity for Pd_3Cl^+ (Figure 2) lies in stark contrast with the textbook mechanism for conventional Pd^0-catalyzed Suzuki−Miyaura cross couplings, which begins with oxidative addition of an organo(pseudo)halide to a mononuclear Pd^0 center, followed by transmetalation and reductive elimination steps. These results indicate that Pd cluster catalysis may operate in a way different from that of conventional Pd catalysts. Indeed, such distinctive reactivity

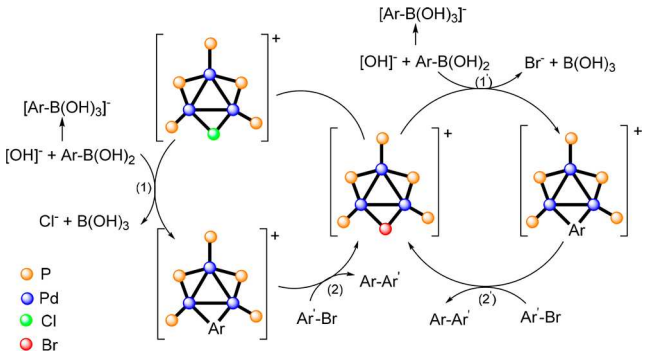

Figure 2. Proposed mechanism of an SMCC reaction catalyzed by $Pd_3Cl{\cdot}SbF_6$. After one cycle the species Pd_3Br^+ is formed and becomes the catalyst for further cycles, as confirmed by using this complex as the starting catalyst. Reproduced from ref 19. Copyright 2017 with permission from American Chemical Society.

could potentially be exploited in cross-coupling catalysis. Fairlamb and co-workers showed that $[Pd_3(\mu\text{-X})(\mu\text{-PPh}_2)_2(PPh_3)_3]^+$ could be generated *in situ* by simply exposing the $Pd(OAc)_2/2PPh_3$ precatalyst system to a suitable organohalide; therefore, such reactivity could be accessed without having the synthetically challenging Pd_3 cluster synthesis (*vide supra*). That such Pd_3 clusters can be formed *in situ* from the simple $Pd(OAc)_2/2PPh_3$ precatalyst system highlights the potentially broader significance of these species.

The groups of Malacria and Maestri have closely investigated the remarkable hydrogenative catalytic activities of $[Pd_3(\mu\text{-SR})_3(PR_3)_3]^+Y^-$ (Figure 3), which have been shown to vary as a function of structure.[53] The $[Pd_3(\mu\text{-SR})_3(PR_3)_3]^+Y^-$ cluster motif, when it is employed as a catalyst for the chemo- and stereoselective semireduction of alkynes, can be used in lower loadings and with higher catalyst stabilities than the previous state-of-the-art catalyst. The structure of this complex can be compared and contrasted with that of Coulson's $[Pd_3(\mu\text{-X})(\mu\text{-PR}_2)_2(PR_3)_3]^+Y^-$ structure (*vide supra*). Both feature an approximately equilateral cationic Pd_3 core bridged by three anionic ligands and capped by neutral phosphine ligands, resulting in an average oxidation

https://doi.org/10.1021/acscatal.2c03345
ACS Catal. 2022, 12, 11615−11638

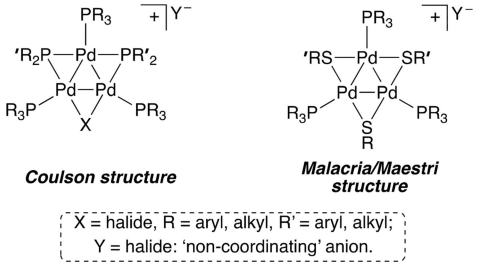

Figure 3. Structural comparison between tripalladum cluster complexes: $[Pd_3(\mu\text{-SR})_3(PR_3)_3]^+Y^-$ and $[Pd_3(X)(PR'_2)_2(PR_3)_3]^+Y^-$.

state of 4/3 per Pd. Instead of two phosphide and halide bridging ligands, however, three anionic organosulfido bridging ligands are present and, as a result, the core structure of $[Pd_3(\mu\text{-SR})_3(PR_3)_3]^+Y^-$ is C_3 symmetric. The complex has been electronically and sterically tuned by varying both the tertiary organophosphine and organosulfido substituents, for optimal catalyst activity. Theoretical and experimental studies have demonstrated that the Pd_3 triangular core displays d-orbital aromaticity, which has been postulated to account for its unusual activity; for example, the d-orbital system is able to interact with Lewis acidic metal cations (See section 3 for further details).[54,55] In addition to the Lewis base character of Pd_3 clusters, the $[Pd_3(\mu\text{-SR})_3(PR_3)_3]^+Y^-$ cluster complexes were described as being oxygen- and moisture-stable.[56]

The first-generation cluster catalysts, adopting the $[Pd_3(\mu\text{-SR})_3(PR_3)_3]^+$ motif, which were substituted with varying electron-withdrawing and electron-donating ligand fragments, were successfully employed as versatile catalysts for the selective semireduction of internal alkynes to *cis*-alkenes under transfer hydrogenation conditions (Scheme 9), avoiding the formation of the undesired *trans*-alkene, terminal alkene, and the over-reduced alkane products.[21] A range of cluster analogues featuring various organophosphine and organosulfido substituents were subsequently synthesized and tested in transfer hydrogenation catalysis. The screening of the different catalysts synthesized showed that more electron deficient groups increased the internal *cis*-alkene selectivity, albeit reducing the catalyst reactivity, giving rise to lower yields of the products.

Later studies on the factors influencing the electronic and structural properties of Pd_3 clusters allowed an optimized catalytic system for transfer-hydrogenation reactions to be identified, allowing delivery of an internal *cis*-alkene with almost complete selectivity using a low catalyst loading (0.03 mol %).[20] The enhanced second generation of Pd_3 cluster complexes featured a water-solubilizing sulfonate-substituted triphenylphosphine ligand, resulting in a zwitterionic structure containing the noncoordinating anion (Scheme 10). Among

Scheme 10. Synthetic Route for Second Generation of Zwitterionic Pd_3 Complexes, Bearing One Zwitterionic Sulfonated Triphenylphosphine, Two *p*-Tolylphosphines, and Bridging Methylthiolates (Top) and the Pd_3 Cluster VIII Catalyzing the Semireduction of Phenylpropyne to *cis*-1-Phenylpropene under the Employed Reaction Conditions (Bottom)

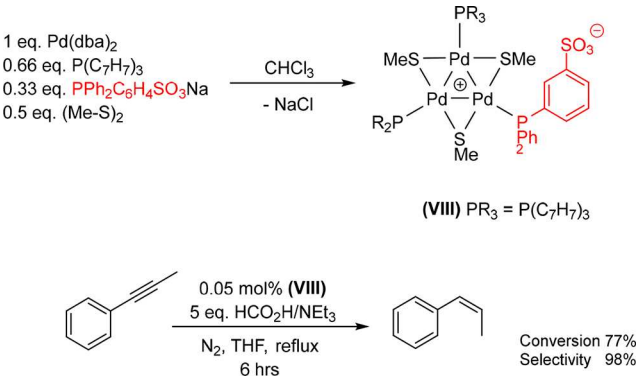

the assessed Pd_3 clusters, one containing a zwitterionic monosulfonated triphenylphosphine, two terminal tri-*p*-tolylphosphines, and two bridging methyl sulfides showed the highest conversion to the *cis*-alkene stereoisomer (Scheme 10).

All of the synthesized zwitterionic Pd_3 complexes, each containing two of a range of relatively electron donating and electron withdrawing triphenylphosphine substituents along with one zwitterionic monosulfonated triphenylphosphine, were shown to be more active but less selective catalysts for the semihydrogenation of internal alkynes, compared to the first generation of $[Pd_3]^+$ complexes. It was suggested that due

Scheme 9. Pd_3-Catalyzed Selective Semireduction of Alkynes to *cis*-Alkenes under Transfer Hydrogenation Conditions[a]

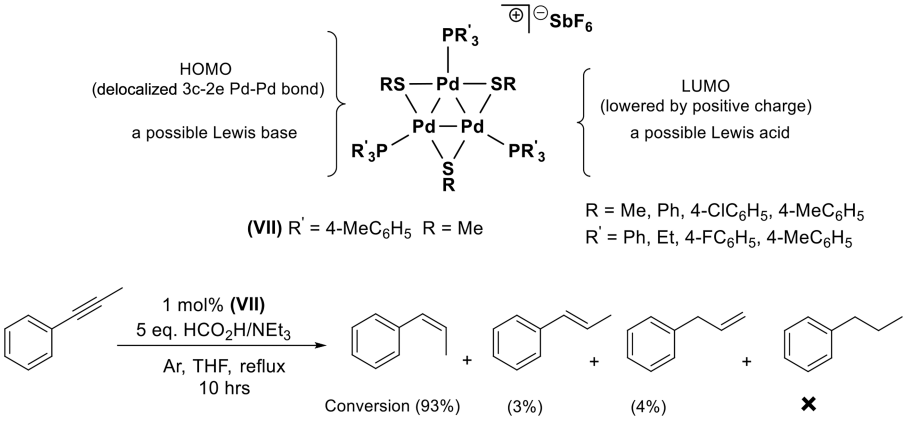

[a]Using tri-*p*-tolylphosphine as terminal ligands and methyl sulfide as bridging ligands delivered the most efficient precatalyst; no trace of alkyl product was observed.

https://doi.org/10.1021/acscatal.2c03345
ACS Catal. 2022, 12, 11615−11638

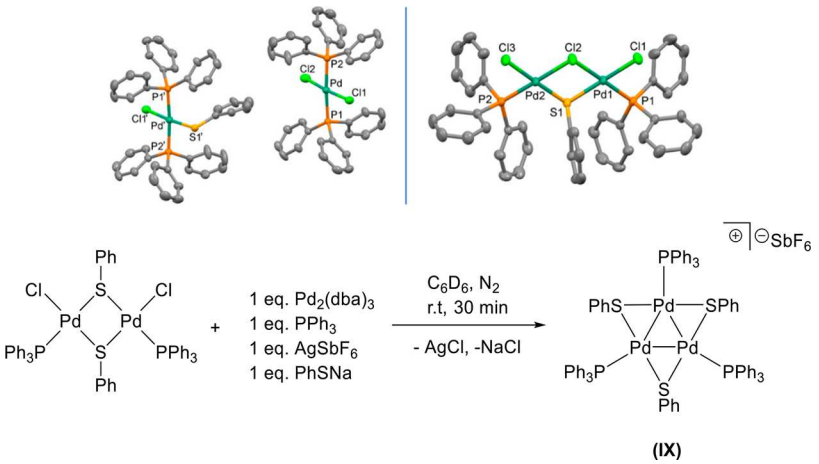

Figure 4. Molecular structure of $[Pd(SPh)(PPh_3)_2Cl][Pd(PPh_3)_2Cl_2]$ (top left) and of $[Pd_2(\mu\text{-}SPh)(\mu\text{-}Cl)(PPh_3)_2Cl_2]\cdot CHCl_3$ (top right). Reaction of *cis*-$[Pd^{II}(\mu\text{-}SPh)(PPh_3)Cl]_2$ with Pd^0 in the presence of phosphine ligand resulted in the formation of **IX** (bottom). Reproduced from ref 58. Licensed under ACS AuthorChoice.

Scheme 11. Cycloisomerization Reaction of Terminal 1,6-Enynes, Catalyzed by 1 mol % of Pd_3 Complex under the Employed Reaction Conditions and an Inert Atmosphere

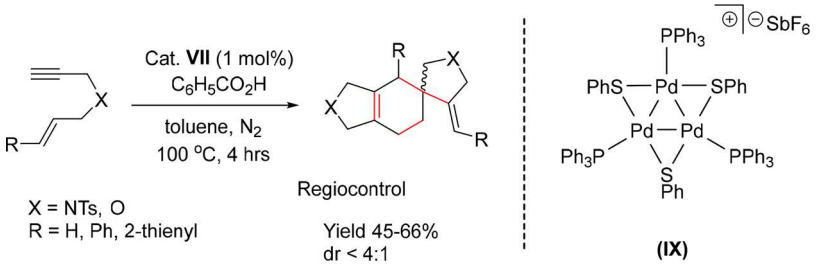

to a *trans*-like effect from the anionic ligand in the structure of the zwitterionic cluster, the phosphine ligands on the opposite edge of the Pd_3 triangle would be more labile, facilitating approach of the alkyne substrate to the Pd_3 catalyst.[20] Destabilization is induced by π-donation of the electron density to the ligand antibonding orbitals *trans* to the anionic ligand, a phenomenon supported by DFT calculations. The reasoning for the reduced selectivity was not discussed in this case. The formation of Pd black during the reaction suggested that these catalysts are less robust than their cationic analogues, due to ligand lability. Monitoring the concentration of zwitterionic catalyst **VIII** during the semireduction reaction by UV−visible spectroscopy showed that the absorption bands for the cluster remain clearly visible and relatively unchanged throughout the reaction, indicating the structural stability of Pd_3 cluster throughout the catalytic hydrogenation reaction process. Hence, the notion was supported that the triangular Pd_3 cluster acts as the likely active catalyst, rather than converts into another species *in situ*. This study indicated that the addition of excess phosphine ligand inhibits the generation of the Pd_3 cluster and results in the formation of monomeric and dimeric Pd^{II} complexes (Figure 4, top).[57] To explore the mechanism behind the transformation to Pd_3 complexes, the Pd^{II} dimer species *cis*-$[Pd^{II}(\mu\text{-}SPh)(PPh_3)Cl]_2$ was reacted directly with $Pd_2(dba)_3$ and 1 equiv of phosphine ligand, which resulted in the formation of the Pd_3 complex $[Pd(\mu\text{-}SPh)(PPh_3)]_3^+$ (**IX**) (Figure 4 bottom).[58]

Formation of **IX** from the reaction shown in Figure 4 supported the hypothesis that either the chlorinated solvent facilitates the oxidation of the Pd^{II} precursor through a single-electron-transfer (SET) process or that the oxidation of the Pd^0 starting material occurs onto the coordinatively unsaturated *cis*-$[Pd^{II}(\mu\text{-}SPh)(PPh_3)Cl]_2$, resulting in the formation of delocalized three-center−two-electron bonds.[58−60] The catalytic reactivity of **IX** is shown in Scheme 10. In this study, the reactivities of the monomeric Pd species $[Pd(PPh_3)_2(SPh)Cl][Pd(PPh_3)_2Cl_2]$, *cis*-$[Pd^{II}(\mu\text{-}SPh)(\mu\text{-}Cl)(PPh_3)_2Cl_2]$, and *cis*-$[Pd^{II}(\mu\text{-}SPh)(PPh_3)Cl]_2$ (all shown in Figure 4) were each tested in a solvent-free hydrogenation of phenylpropyne under conditions similar to those shown in Scheme 10 by adding 0.09 mol % of the additive tri-*p*-tolylphosphine ligand and using 0.03 mol % catalyst loading. Of the phosphine ligands tested as additives—required to boost conversion and selectivity—tri-*p*-tolylphosphine was found to have the highest positive effect on conversion and selectivity. It was reasoned that an excess amount of ligand could avoid degradation/aggregation of active catalytic species, particularly when the concentration of substrate(s) decreases—the formation of black particulate material after catalysis was minimized with excess ligand. In contrast, when the monomeric Pd species $[Pd(PPh_3)_2(SPh)Cl][Pd(PPh_3)_2Cl_2]$, *cis*-$[Pd^{II}(\mu\text{-}SPh)(\mu\text{-}Cl)(PPh_3)_2Cl_2]$, and *cis*-$[Pd^{II}(\mu\text{-}SPh)(PPh_3)Cl]_2$ were employed as the catalysts, the presence of black particles was observed, even in the presence of excess ligand. In all cases, the reactivity of the mono- and dinuclear Pd^{II} species was proven to be lower than that of **IX** in the same reaction, although the product selectivity was replicated in all cases. This work indicates that when the related intermediate complexes are employed as catalysts, along with the observation that the $[Pd(\mu\text{-}SPh)(PPh_3)]_3^+$ cluster remains intact throughout the catalytic

https://doi.org/10.1021/acscatal.2c03345
ACS Catal. 2022, 12, 11615−11638

Scheme 12. Generalized Scheme Showing the Scope of Reactivity of *para*-Substituted Phenyl Iodides with Phenylboronic Acid, Enabled by the Pd_3^+ Cluster Catalyst $[Pd_3(\mu\text{-}S(p\text{-}Cl\text{-}C_6H_4)_3(P(p\text{-}F\text{-}C_6H_4)_3]^+[SbF_6]^-$

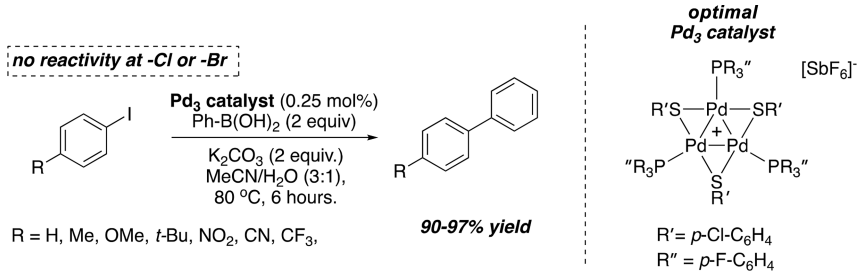

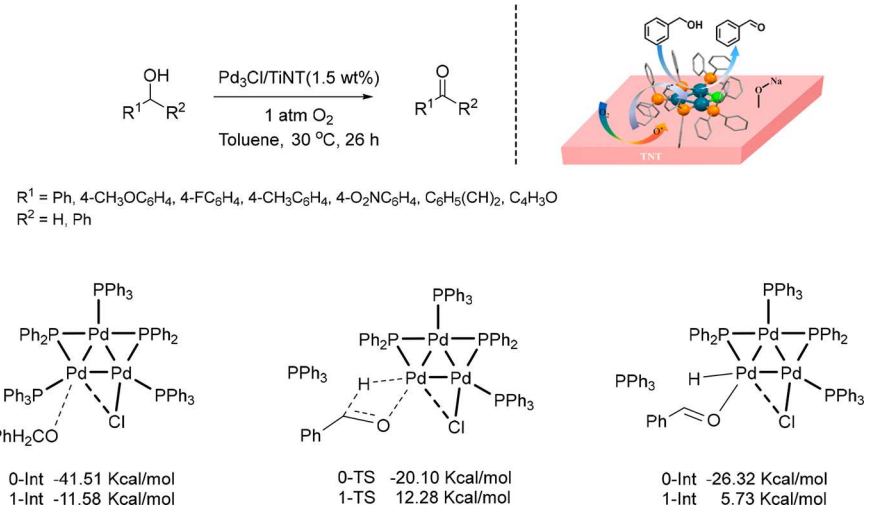

Figure 5. (top) Oxidation reaction of alcohols to the corresponding ketones catalyzed by $[Pd_3(\mu\text{-}Cl)(\mu\text{-}PPh_2)_2(PPh_3)_3]^+$. At the top right is a representation of catalysis during the turnover. (bottom) Potential energy for the reaction intermediates and transition states in the α-C−H abstraction step in both the 0 and +1 oxidation state of the cluster. Adapted with permission from ref 65. Copyright 2018 Wiley-VCH.

semireduction reaction, convergence on a common active catalyst occurs under the hydrogenative conditions.

The related $[Pd_3(\mu\text{-}SMe)_3(PPh_3)_3]^+$ complex was also successfully applied to diastereoselective cycloisomerization reactions of terminal 1,6-enynes and internal dienynes to form tricyclic cyclohexene architectures under mild reaction conditions, enabled by carboxylic acid additives (see the generalized Scheme 11).[22,61,62]

When common Pd catalyst precursors such as $Pd(OAc)_2$, $Pd_2(dba)_3$, and $Pd(PPh_3)_4$ were employed as catalysts under similar conditions, no cycloisomerized product was formed. In a later study it was shown that, when a catalyst with a stronger σ-donating phosphine ligand was employed such as PEt_3 instead of PPh_3, it attenuated the cyclization reactivity.[61] It was hence reasoned that phosphine dissociation is required for substrate (i.e., alkyne) coordination, a conclusion supported by the observation that, when the cycloisomerization catalysis was carried out with an excess of phosphine ligand (PPh_3), the reactivity was vastly reduced and an induction period measured.

Liu and co-workers synthesized a range of $[Pd_3(XPh)_3(PAr_3)_3]^+[SbF_6]^-$ derivatives (X = S, Se), including those with novel bridging selenide groups in place of sulfide groups.[63] In this study, these C_3-symmetric catalysts were tested for the first time in SMCC reactions. While the complexes were able to efficiently activate substituted aryl and heteroaryl iodides for reactions with phenylboronic acids (Scheme 12), the Pd_3 clusters could not enable such reactivity at less activated aryl bromides or chlorides under the conditions tested. This observation constitutes an interesting result, as structurally comparable $[Pd_3(\mu\text{-}Cl)(PR_2)_2(PR_3)_3]^+Y^-$ clusters have been shown to be highly active at aryl bromide sites at low catalyst loadings. This observation might further validate the proposed catalytic role of the μ-Cl site of the $[Pd_3(\mu\text{-}Cl)(PR_2)_2(PR_3)_3]^+Y^-$ type clusters (*vide supra*).

While investigating the cross-coupling reaction of borylzincs with organohalides for the synthesis of complex organoboranes, Aldridge et al. discovered that the Coulson-type Pd_3 cluster $[Pd_3(\mu\text{-}Br)(\mu\text{-}PPh_2)_2(PPh_3)_3]^+[Zn_6Cl_{15}]_3^-$ was isolated, in this case assigned as a intermediate en route to the reduced and activated catalytic species, arising from the commonly deployed precatalytic source $PdCl_2(PPh_3)_2$. A borylzinc species acted as a reductant to produce the monomeric species $Pd(PPh_3)_2$ and the cluster complex, the ratio of which varied as a function of Pd:Zn ratio: the fewer equivalents of the reductant, the higher the proportion of Pd cluster to P monomer.[64]

A later study by Zhu et al. focused on structural aspects of a titania nanotube (TiNT) supported Coulson-type Pd_3 cluster, $[Pd_3Cl(PPh_2)_2(PPh_3)_3]^+X^-$, and its applications in the catalytic oxidation of primary and secondary alcohols to aldehydes and ketones, respectively (Figure 5).[65] It was suggested that possible charge transfer between the support and the metal played a role in boosting the catalytic activity of the system. Pd_3Cl/TiO_2 nanotubes (TiNT) were successfully applied in the aerobic oxidation of primary and secondary

https://doi.org/10.1021/acscatal.2c03345
ACS Catal. 2022, 12, 11615−11638

Scheme 13. Reagents and Conditions Used by Zhu et al. for the Selective Hydrogenative Formation of Benzalaniline from Nitrobenzene and Benzaldehyde, Enabled by the γ-Al_2CO_3-Supported, Coulson-Type Pd_3Cl^+ Catalyst $[Pd_3(\mu\text{-}Cl)(\mu\text{-}PPh_2)_2(PPh_3)_3]^+$ [a]

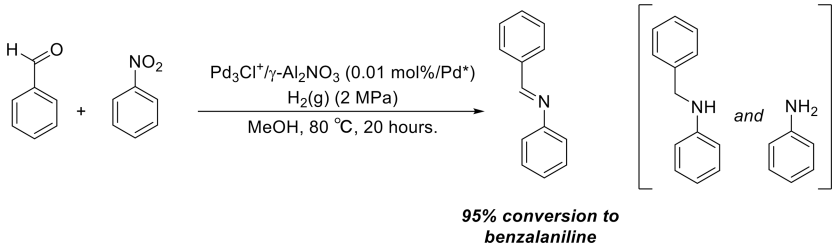

[a]The asterisk indicates that the amount was calculated by the authors of this work based on reported reagent and catalyst loading and catalyst Pd wt %.

Scheme 14. Synthetic Method for the Synthesis of a Catalytically Active Silyl-Phosphido Ligated Pd_3 Cluster from $[Pd^0(CNt\text{-}Bu_3)_2]$ [a]

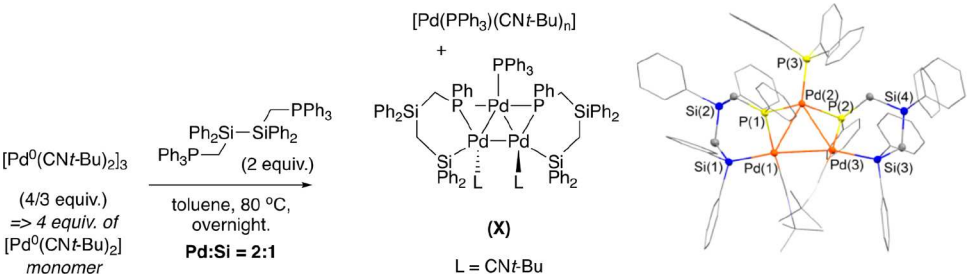

[a]Adapted with permission from ref 67. Copyright 2021 American Chemical Society.

alcohols to the corresponding aldehydes with excellent yields and full selectivity without using a base under the employed reaction conditions.

Analytical methods such as matrix-assisted laser desorption/ionization mass spectroscopy (MALDI-MS), UV−vis, X-ray diffraction (XRD) analysis, and TEM images indicated that the structure of the Pd_3Cl^+ cluster in Pd_3Cl/TiNT remained intact during catalysis. The study investigated the detection of a metal−support interaction from both kinetic and thermodynamic aspects, since neither the homogeneous Pd_3Cl^+ cluster nor the TiNT support could effectively catalyze the aerobic oxidation reaction under the same conditions. It was proposed that cationic Pd_3Cl^+ is strongly attracted to oxygen vacancy sites; therefore, electrons from the vacancy could be transferred to Pd_3Cl^+ and facilitate the oxidation reaction of alcohols, as observed by XPS analysis. Therefore, $[Pd_3(\mu\text{-}Cl)(\mu\text{-}PPh_2)_2(PPh_3)_3]^0$ (denoted Pd_3Cl^0), with an overall oxidation state of 0, was suggested to be the active catalytic species facilitating the oxidation reactions. DFT calculations for the β-H elimination step, which was accepted to be rate-eliminating, confirmed that the energy barrier for the overall transformation for Pd_3Cl^0 is exothermic by 39.7 kcal/mol, whereas the overall transformation for Pd_3Cl^+ is endothermic by 5.7 kcal/mol (Figure 5), in broad agreement with results obtained from XPS.

Another synthetic use of supported catalytic Coulson-type clusters was reported by Zhu et al.[66] In this case, a $[Pd_3(\mu\text{-}Cl)(\mu\text{-}PPh_2)_2(PPh_3)_3]^+$ (Pd_3Cl^+) cation was tethered to an optimized γ-Al_2O_3 support to enable highly efficient and selective one-pot formation of benzalaniline by selective reductive coupling of simple benzaldehyde and nitrobenzene in the presence of H_2. The process avoided the undesired benzylaniline and aniline side products (Scheme 13).

The unsupported Pd_3 cluster was competent in the model reaction; however, it was found to be not as selective for the valuable benzalaniline (imine) product in comparison with the γ-Al_2CO_3-supported versions. The Pd_3Cl^+-supported catalyst performed better than PdNPs (~2−3 nm) on γ-Al_2O_3, SiO_2, and TiO_2 supports in the model reaction. Pd/C was reported to simply form the less valuable benzylaniline (amine) product. Notably, the γ-Al_2CO_3-supported Pd_3Cl^+ catalyst could be recycled (at least once, as reported) without loss of activity. Furthermore, minimal leaching of Pd into the reaction solution was observed, as determined by ICP-MS from the postreaction solution. A UV−visible spectroscopic analysis of the catalyst before and after catalytic use showed no discernible change, which was taken to indicate that the supported cluster species could mediate the transformation without undergoing a speciation change. The observation of different chemoselectivities when the solid support is changed is striking, as it suggests that the solid support can interfere, constructively in this case, with catalytic activity and further probing reasons for these differences is therefore of interest.

Sunada and Usu reported that the reaction of $[Pd^0(CN\text{-}t\text{-}Bu)_2]_3$ (itself a Pd_3 cluster, with a valence-electron count of 36) with a disilane compound resulted in formation of the triangular Pd complex **X** (Scheme 14).[67] The product cluster **X** bears analogy with the Coulson motif (*vide supra*), as it is a 44-electron complex featuring an overall oxidation state of 4/3, two anionic μ-phosphido ligands, and a capping distal PPh_3 ligand. Notable differences are that the overall complex is neutral due to two bidentate, dianionic μ-phosphidodiphenylsilyl ligands and two neutral isocyanide ligands. Cluster **X** was tested as a catalyst in an SMCC reaction (2 mol %, with respect to Pd loading) between 4-bromoacetophenone and 4-methoxyphenylboronic acid, providing the cross-coupled

https://doi.org/10.1021/acscatal.2c03345
ACS Catal. 2022, 12, 11615−11638

product in quantitative yields. No comparison was presented for the relative catalytic activity of trinuclear cluster **X** against its Pd^0 precursor complex $[Pd^0(CN\text{-}t\text{-}Bu)_2]_3$ or the side product of the synthesis: $[Pd^0(PPh_3)(CN\text{-}t\text{-}Bu)_n]$.

Indeed, the Pd_3 cluster $[Pd^0(CN\text{-}t\text{-}Bu)_2]_3$ has been shown to act as a precursor to many diverse isocyanide-ligated Pd cluster complexes, thus supporting the notion that the electron-withdrawing effect of the isocyanide ligand may allow stabilization of well-defined ligated clusters over the formation of Pd black.[68−70]

Sunada et al. also synthesized a Pd_4 cluster by reactions between $[Pd^0(CNt\text{-}Bu)_2]$ and substituted cyclotetrasilanes, forming a hexagonal planar core structure with a central Pd atom surrounded by alternating Pd and Si atoms (**XI**; Scheme 15, top). Each edge Pd was additionally stabilized by a CN-*t*-Bu ligand.[71,72] The Pd_4 cluster demonstrated good activity as a catalyst for the hydrogenation of alkenes and alkynes.

Scheme 15. Synthesis of Catalytically Active Pd_4 Cluster Complexes

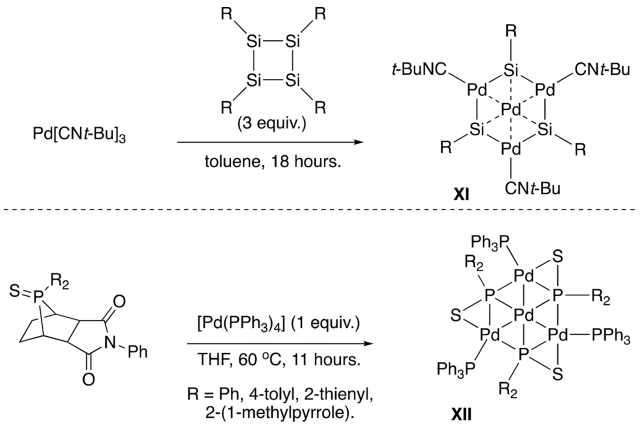

Duan, Mathey et al. found that a well-defined Pd_4 complex could be synthesized by treatment of $[Pd(PPh_3)_4]$ with a 7-phosphororbornene sulfide (**XII**; Scheme 15, bottom).[73] The solid-state structure was interrogated by X-ray crystallographic analysis and found a solid-state structure featuring a "star-like" pyrimidal Pd_4 core, stabilized by phosphinidene sulfide ligands and capping triphenylphosphine ligands. The complex was shown to be highly resistant to chemical reduction and ligand substitution. Crucially, **XII** was catalytically compentent in simple cross-coupling reactions of phenylboronic acid with both iodobenzene and chlorobenzene, at relatively low catalyst loadings (0.1 mol %).

Kurosawa et al. discovered that the direct reaction between $[Pd_2(dba)_3]$ and tetraphenylphosphonium chloride in the presence of $[C_7H_7]^+[BF_4]^-$ afforded the Pd_3 cluster complex $[PPh_4]^+[Pd_3Tr_2Cl_3]^-$ (**XIII**), which features a central, chloride-capped triangular Pd_3 anion, sandwiched between two cycloheptatrienyl (Tr) cations (Figure 6).[74,75] Later it was found that a related, well-defined aryl-sandwiched complex (**XIII**) could catalyze the intramolecular cyclization reaction between 2-phenylethynylaniline to 2-phenylindole (Figure 6), while the classic Pd catalytic precursors $[Pd^0{}_2(dba)_3]$ and $[Pd(OAc)_2]$ could not.[76]

Ma et al. discovered that the sulfide-bridged cluster that had been studied by Malacria and Maestri (*vide supra*) could be incorporated into an anionic metal−organic framework (MOF) (Figure 7).[77] The authors sought to take advantage of the porous (and hence high surface area), tunable nature of the MOFs bioMOF-200-1 and bioMoF-100-2 to enhance the efficiency of catalytic transfer semihydrogenation reactions of internal alkynes. The MOF-supported Pd_3 clusters were prepared simply, by exchange of the cluster $[SbF_6]^-$ counter-anion with the anionic MOF of interest at room temperature. Incorporation was reasoned by quantifying the amount of displaced cations. However, this does not rule out that some of the Pd cluster could have been bound to the MOF surface. When it was applied to model transfer-hydrogenation reactions of diphenylacetylene and methylphenylacetylene, the MOF-supported Pd_3 cluster showed high selectivity (>94%) toward to the (*Z*)-alkene over the (*E*)-alkene or the alkane products, comparable to that of the according unsupported Pd_3 cluster.

A comparative catalyst (Pd) loading of the MOF-supported catalyst was not given in the study,[77] thus precluding a catalyst efficacy analysis between the MOF-supported and -unsupported catalysts. Recyclability tests showed each MOF to be recyclable at least twice, with a slight (5−10%) loss in activity of the MOF-supported catalyst after each run. Leaching experiments (filtration test) indicated that the presence of the heterogeneous MOF material was required for catalysis and

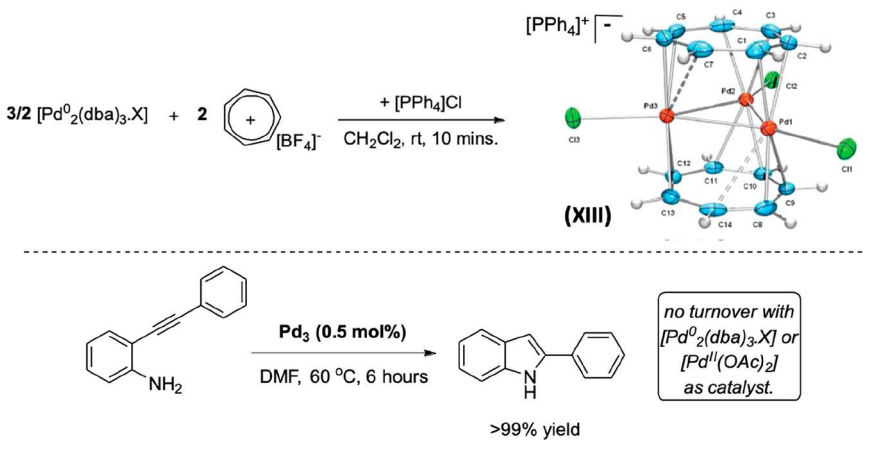

Figure 6. Schemes showing the synthesis of the cycloheptatrienyl Pd_3 sandwich complex $[PPh_4]^+[Pd_3Tr_2Cl_3]^-$ (top) and its application as a catalyst in a cycloisomerization reaction forming 2-phenylindole under the employed reaction conditions (bottom). Adapted with permission from ref 74. Copyright 2006 American Association for the Advancement of Science.

https://doi.org/10.1021/acscatal.2c03345
ACS Catal. 2022, 12, 11615−11638

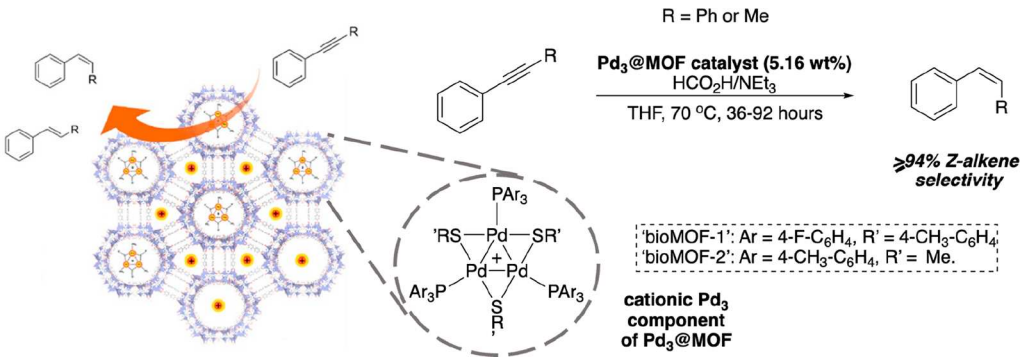

Figure 7. (left) Depiction of the bioMOF structure, showing the structures of the two encapsulated Pd_3^+ species used in this study. (right) Model conditions used for analysis of the Pd_3@MOF as a catalyst for selective transfer-hydrogenation reactions. Adapted with permission from ref 77. Copyright 2021 American Chemical Society.

was not merely a source of solution Pd species. Accordingly, the powder XRD patterns from the catalytic material did not appreciably change after each recycling experiment.

2.3. Interface between Small Clusters and Nanoparticles. Given that well-defined Pd_n clusters have been shown to form from simple precatalytic Pd sources and from clustering of Pd dimer species, the relevance of this needs to be placed in the context of what the field knows about Pd speciation in general—particularly with respect to complex homogeneous and heterogeneous behavior. Below, to this end, we have compiled a short nonexhaustive review on Pd speciation and interconversion between homogeneous and heterogeneous catalytic manifolds. Further comprehensive reviews on this topic have also been described.[78−80]

2.3.1. Evidence for Quasi-Heterogeneous/Heterogeneous Behavior in Cross-Coupling Catalysis. In recent years various strands of evidence have been reported that support the heterogeneous behavior of active Pd in some cross-coupling reactions. In 2010 Fairlamb et al. investigated the catalytic competence of polyvinylpyrrolidone (PVP)-stabilized PdNPs in a range of different sizes (1.8−4 nm; truncated cuboctahedra) in SMCC reactions between iodobenzene and arylboronic acid in alcoholic solvents, under mild reaction conditions.[11] It was shown that the cross-coupling efficacy (TON) was correlated with the number of defect sites present (as measured by TEM) on the surface. EXAFS was employed to monitor the coordination environment at the PdNP surface, which indicated no measurable morphological change at the Pd surface during the reaction turnover; minimal leaching was seen to occur. Moreover, a kinetic analysis of the reaction showed no induction period, with standard tests suggesting a heterogeneous reaction behavior. Xie et al. also utilized Au−Pd core−satellite superstructures (silica particles coated with a layer of AuNPs and an outer layer of PdNPs) that were surface-modified with 4-bromothiophenol, which was tethered via a sulfide linker to the Pd surface outer layer of the nanoparticle.[81] The number of defect sites and morphology type have been proven to be key to the activity of Pd nanoparticles.[82,83] The tethered substrate was able to be cross-coupled in SMCC reactions with phenylboronic acid (in aqueous K_2CO_3), forming a tethered biaryl product, as determined by surface-enhanced Raman spectroscopy (SERS). Although leached Pd was detected, appropriate control experiments showed this material to be catalytically inactive. It should be stated that it is plausible that the leached Pd may have changed to an inactive form upon separation from the initial catalyst mixture. Taken together, this work provided further evidence that aryl halides could be activated and cross-coupled with arylboronic acids on the surface of a nanoparticle: i.e., exhibiting true heterogeneous behavior.

On the other hand, there have been numerous published examples of cross-coupling catalysis with homogeneous species leached into the solution phase from heterogeneous sources being responsible for catalysis. Rothenberg et al. demonstrated leaching of catalytically active Pd from relatively large nanoparticles (∼15 nm), which had been generated from *in situ* reduction of $[Pd(NO_3)_2]$ in the presence of a stabilizing tetra-*n*-octylammonium glycolate salt.[84] By designing a bespoke reactor containing a porous membrane that would only allow passage of smaller particles (<5 nm), it was proved that leached species can be active in cross-coupling processes. This finding, however, was not taken to necessarily confirm that the leached species are operating exclusively as mononuclear Pd catalyst species, since nanoparticles of this size could theoretically contain as much as several thousand Pd atoms (depending on their shape).[11a,b] Thus, the reaction could still be occurring on a surface of leached clusters. Zeng et al. designed a core−shell FeO support for PdNPs, surrounded by a microporous silica membrane, in order to preclude interactions between larger substrates and the PdNP surfaces prior to catalyst turnover in an SMCC reaction.[85] It was hence determined under their conditions that oxidative addition of the iodobenzene substrate onto the heterogeneous surface caused etching of active Pd and, as a result, leaching of Pd occurred in the subsequent C−C bond-forming steps proceeding in the solution phase. Redeposition of recycled Pd^0 onto the heterogeneous catalyst surface after complete conversion of iodobenzene substrate allowed for efficient catalyst recycling. Such a leaching−redeposition mechanism has been described as "quasi-heterogeneous" catalysis.

Glorius and co-workers discovered that direct C−H arylation of variety of heterocycles with diaryliodonium salts could be mediated by species leached from a Pd supported on carbon (Pd/C) precatalyst, which was found to act via a quasi-heterogeneous mechanism (Scheme 16).[86]

While highly oxidizing conditions were employed where leaching could be expected, the standard heterogeneity tests indicated heterogeneous catalysis. A heterogeneous catalytic manifold in this case was supported by subsequent XPS, XANES, and XAFS analysis, which found that a PdNP surface is functionalized by phenyl groups (transferred from the diaryliodonium salt substrate) and oxygen (from H_2O) under

https://doi.org/10.1021/acscatal.2c03345
ACS Catal. 2022, 12, 11615−11638

Scheme 16. Heterogeneously Catalyzed Functionalization of Heterocycles Using Pd/C as Catalyst and Diaryliodonium Salts under the Employed Reaction Conditions

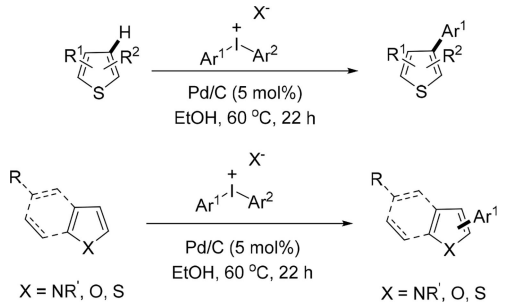

working catalysis conditions. The catalytic system was subsequently applied to the direct arylation of polyaromatic compounds with diaryliodonium salts under similar reaction conditions, which gave rise to good site selectivity, intriguingly often at the most sterically hindered positions.[87] Although the kinetic profile of the model reaction showed an induction period, indicating that the active catalytic species was formed from a precatalyst over time, heterogeneity tests such as a mercury-poisoning test, a three-phase test, and a hot-filtration test pointed toward a heterogeneous catalyst system. With this mechanistic evidence in hand, it is therefore suggested either that a heterogeneous species can mediate transformations by surface catalysis through leaching and redeposition on the surface or that an active homogeneous species forms from the heterogeneous source (Figure 8).

Following the studies on leaching/redeposition mechanism in previously assumed heterogeneous catalysis, a recent work by Scaiano et al. provided evidence for the migration of catalytic palladium species during the reaction through a dissolution/redeposition mechanism after activation of the surface.[88] The PdNPs@TiO_2-catalyzed SMCC reaction of 2-thienylboronic acid and a dibromo-BODIPY-based probe (DB-BODIPY, a fluorescent probe) under flow conditions was studied at a single-molecule level using total internal reflection fluorescence microscopy (TIRFM) (Scheme 17). The reactions, which were monitored under flow conditions, exhibited the localization of the formation of the arylated products in either the presence or absence of a base, although with a significant drop in the reaction yield in the latter. By superimposing the images acquired by TIRFM from the same regions on surface of the catalyst, they found 54% colocalization between the reactant and product, which indicated that the catalytic events occur mostly near the catalyst surface.

Scaiano et al. flowed the reaction mixture over a cover slip coated with PdNPs@Ti_2O and collected product bursts during the exposure time and remeasured the same area after 3 h. Comparing the obtained high-resolution images at different times indicated a displacement of catalytic sites and migration of Pd species, suggested to be atoms or small clusters, to new regions. The study showed that the detachment of catalytic species, as either atoms or small clusters, from the surface of the catalyst could occur and that they could migrate distances of up to 3 mm, generating new heterogeneous catalytic sites to catalyze SMCC reactions under flow conditions.

It is therefore possible that, in each cross-coupling process, an array of different heterogeneous and homogeneous Pd species could be catalytically relevant, as depicted in Figure 9. In a more comprehensive picture, the homogeneous monomeric species could be potentially competing with heterogeneous and quasi-heterogeneous species in the system that each contribute to the reaction, accordingly complicating the reaction kinetic profiles.[89]

2.3.2. Small Clusters: Bridging the Gap between Homogeneous and Heterogeneous Catalysis. The picture in Figure 9 can become complicated by the role of small, ligated Pd_n cluster species, which act to bridge the gap between homogeneous and heterogeneous catalytic manifolds. This is an area that has received relatively little attention in cross-coupling catalysis. A more detailed understanding of the

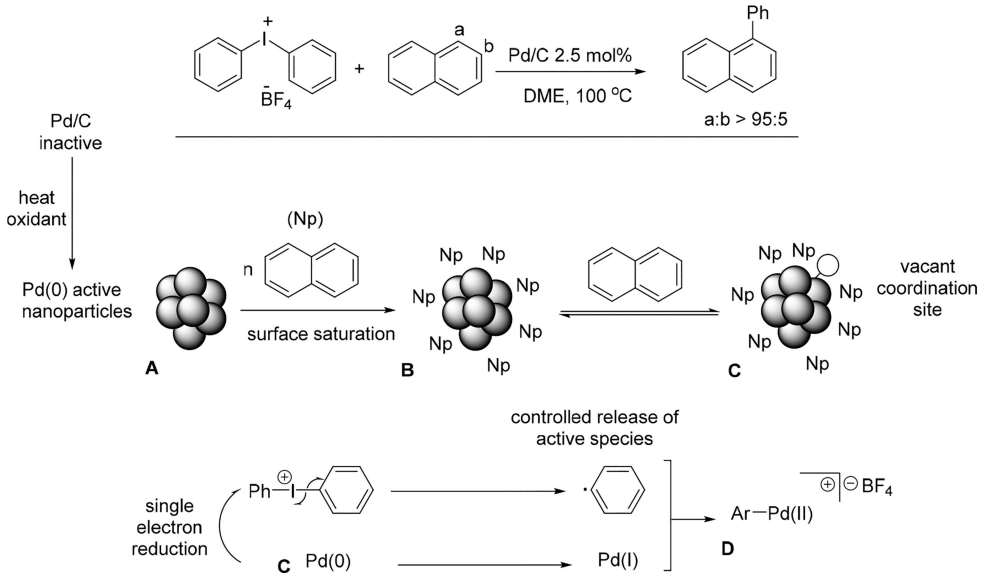

Figure 8. Proposed reaction mechanisms for naphthalene as a representative substrate (Np = naphthalene). Counterions are omitted for clarity when required; treatment of **C** and **D** would be either by electrophilic palladation at a position in naphthalene or by coordination of **D** to the phenyl ring in naphthalene. Reproduced from ref 87.

https://doi.org/10.1021/acscatal.2c03345
ACS Catal. 2022, 12, 11615−11638

Scheme 17. Heterogeneously Catalyzed Pd@TiO_2 SMCC Reaction[a]

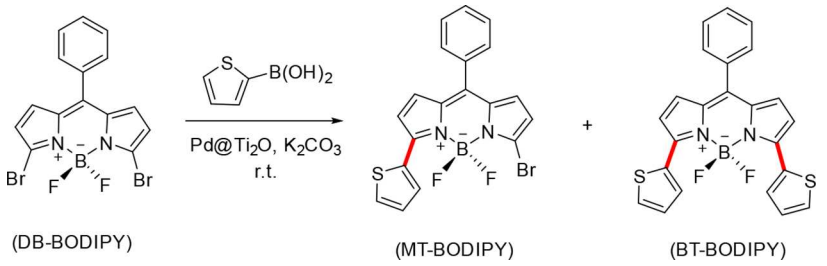

[a]Using a BODIPY-based dibromo substrate as a fluorescence probe giving single- and double-substituted BODIPY-based products under flow conditions, the location of the cross-coupling events were determined and colocalized with the surface of catalytic PdNPs.

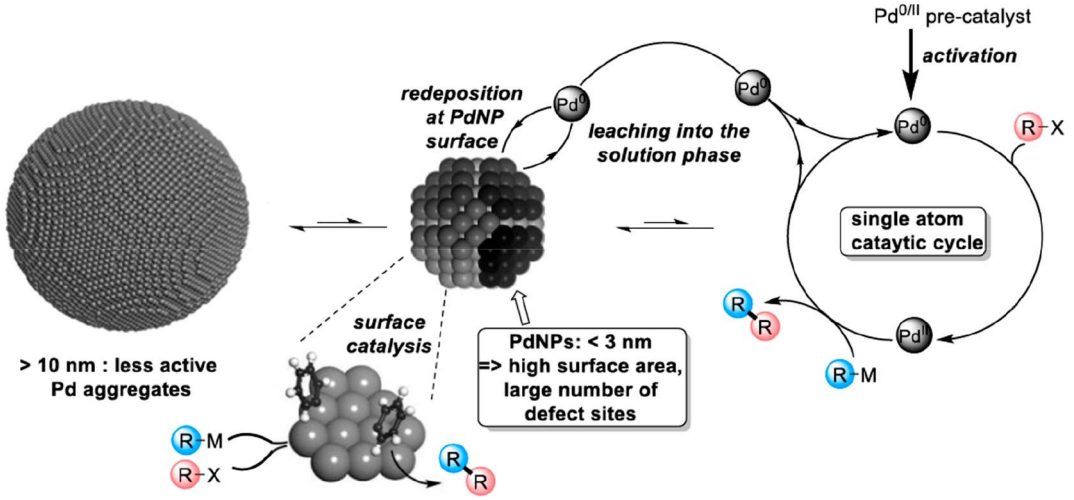

Figure 9. Schematic representation showing the complex picture for the modes of reactivity of homogeneous and heterogeneous metal species in a given cross-coupling process. Adapted from ref 89.

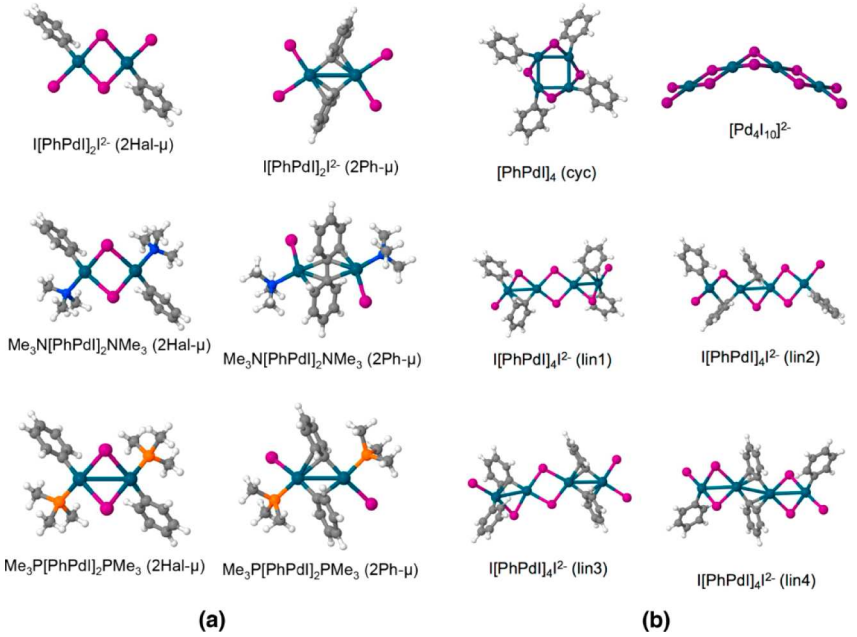

Figure 10. Optimized DFT structures of (a) dimeric Pd intermediates in reactions with PhI and (b) tetrameric Pd intermediates in reactions with iodobenzene. Pd is shown in cerulean, H in white, C in gray, N in blue, P in orange, and I in violet. Reproduced from ref 4. Licensed under ACS AuthorChoice with CC-BY-NC-ND (Creative Commons).

reaction conditions that drive these dynamic processes may allow access to the unique reactivity of Pd_n clusters *in situ*.

The nature of leached Pd species in the form of smaller heterogeneous PdNPs, sub-nanometer palladium clusters, or

https://doi.org/10.1021/acscatal.2c03345
ACS Catal. 2022, 12, 11615−11638

Scheme 18. Proposed Deactivation Pathway for Allylic Substitution Reaction Catalyzed by (1,1-dimethylallyl)Pd(P−P ligand)OTf Complexes, Resulting in Formation of Colloidal Pd

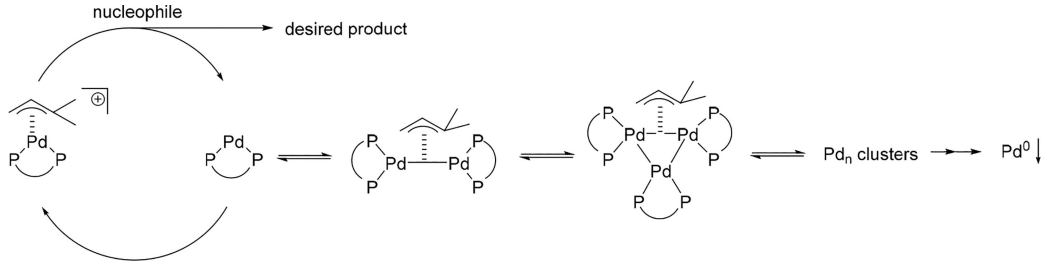

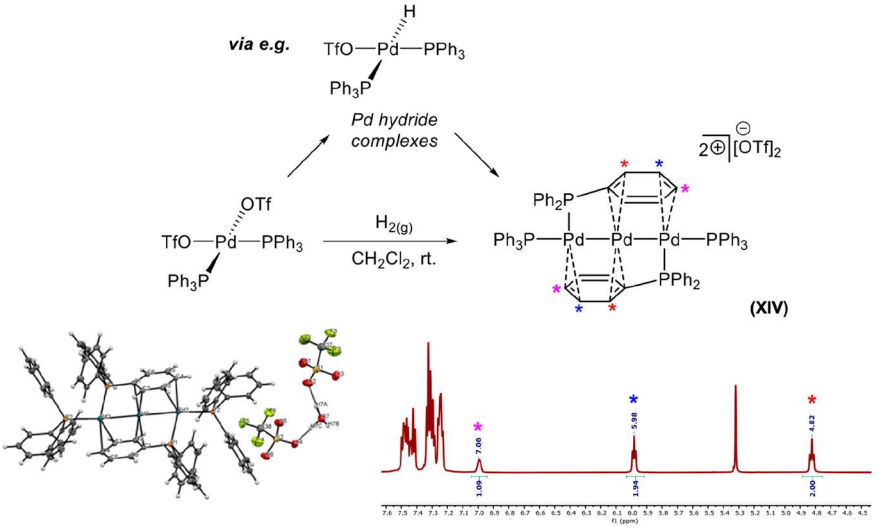

Figure 11. (top) Formation of $[Pd_3(PPh_3)_4][OTf]_2$ (**XIV**) from $[Pd(OTf)_2(PPh_3)_2]$ via Pd hydride complexes (single example given). (bottom left) Single-crystal XRD structure of $[Pd_3(PPh_3)_4][OTf]_2$. (bottom right) ^{1}H NMR spectrum showing assignments of upfield-shifted proton environments in the phenyl ring coordinated to the linear Pd_3 core. Adapted from ref 91.

mononuclear Pd complexes from the catalyst surface has been theoretically investigated by Ananikov et al.[4] A computational study on PdNP speciation resulted in the identification of potential pools of Pd species whose generation could be thermodynamically favored in the course of Pd-catalyzed transformations that involve the oxidative addition of organohalides. It was suggested that ligand binding (L = PMe_3, NMe_3, X^-) and oxidative addition of ArX (X = Br, I) to leached palladium atoms in solution provide a stabilizing energy that can initiate endothermic leaching processes of Pd atoms from the surface of aggregated Pd particles. Moreover, the oligomerization and possible additional ligand binding to the leached Pd species could result in the generation of $[ArPdX]_n$, $X_2[ArPdX]_n^{2-}$, and $L_2[ArPdX]_n$ (n = 1−4), leading to their stabilization in solution (Figure 10). Therefore, the possible formation of Pd_n clusters by oligomerization of soluble species could be thermodynamically favored. However, the authors suggested that the ratio of Pd to ligand present plays a crucial role in Pd_n cluster generation and the subsequent stabilization in the reaction media. This study supports the structure and dynamics of Pd_n clusters in catalytic speciation from a theoretical standpoint.

The nature of the Pd species forming en route to heterogeneous Pd nanoparticles from their corresponding mononuclear complexes has been investigated. For example, Koningsberger et al. presented time-resolved UV−visible and EXAFS spectroscopic evidence for both Pd dimers and trimers forming en route to PdNPs during catalytic turnover, as part of the catalytic deactivation process.[90] In this allylic amination reaction with piperidine and allylacetate, using different (1,1-dimethylallyl)Pd(P−P ligand)OTf complexes, the catalyst deactivation pathway was monitored by excluding the allyl substrate from the stochiometric reaction. The instantaneous formation of a Pd dimer and trimer was observed by addition of piperidine to the reaction mixture, as confirmed by the appearance of related peaks in time-resolved UV−vis spectra and a color change from yellow to red. Fairlamb et al. also reported speciation of a Pd^{II} catalyst in the presence of piperidyl ligand, forming dinuclear $[Pd^0(piperidyl)_n]_2$ in the presence of small quantities of water.[12] Over time, the signals assigned to the Pd dimer and trimer faded away, accompanied by a change of color to dark red and an increasing broad peak at ∼390 nm assigned to larger Pd clusters, resulting in the participation of collodial Pd in the cuvette. The authors suggested that the simultaneous disappearance of dimer and trimer signals maked these species potential intermediates en route to colloidal Pd (Scheme 18).[90]

Recently, Fairlamb, Duckett et al. have structurally characterized a well-defined linear Pd_3 cluster, formed from a simple, electron-deficient Pd^{II} catalyst precursor. The dicationic Pd_3 cluster complex $[Pd_3(PPh_3)_4][OTf]_2$ (**XIV**) was generated from the reaction of *cis*-$[Pd(PPh_3)_2(OTf)_2]$ and H_2 (Figure 11). Pd-monohydride complexes were detected as intermediates in this process.[91] XRD and NMR data both pointed toward the structure being the same in solution as in the solid state: namely, a linear arrangement of the three Pd

https://doi.org/10.1021/acscatal.2c03345
ACS Catal. 2022, 12, 11615−11638

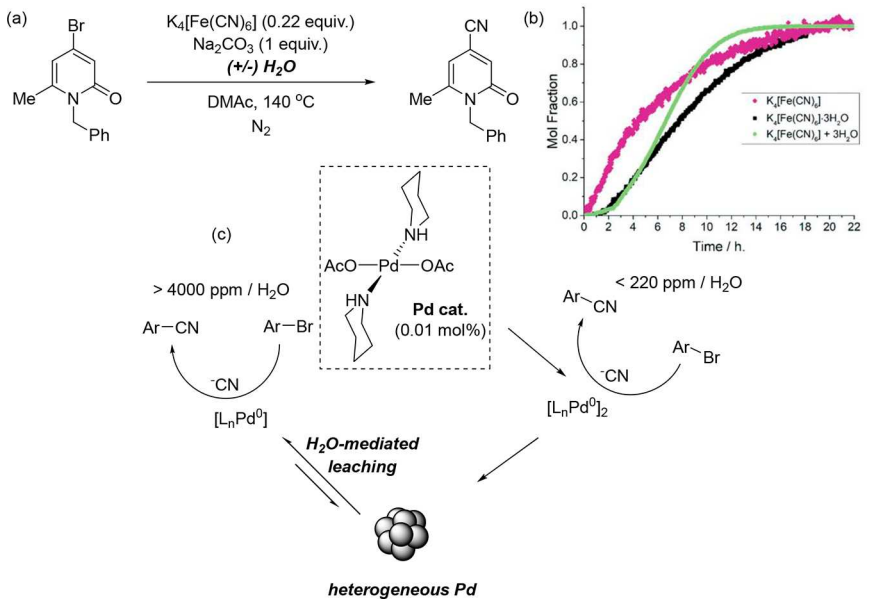

Figure 12. Discoveries regarding the Pd speciation resulting from *trans*-$[Pd(OAc)_2(N\text{-piperidyl})_2]$ during catalytic arylcyanation reactions: (a) reaction conditions used; (b) variation in reaction kinetic profile functions of H_2O present; (c) integrated findings concerning Pd speciation in the presence of different quantities of H_2O. Adapted from ref 12.

atoms, with an average oxidation state of 2/3, stabilized by two capping PPh_3 ligands and two orthogonal PPh_3 ligands, with additional stabilization from π-Ar−Pd interactions. The $AsPh_3$ analogue was also synthesized and characterized. Perhaps unsurprisingly, noting its unique coordination chemistry, the species was found to be unstable in solution, eventually decomposing to form small PdNPs ∼1−3 nm in diameter.

The Pd_3 cluster was shown to be active in hydrogenation and cross-coupling catalysis. In the latter case $[Pd_3(PPh_3)_4][OTf]_2$ (**XIV**) showed selectivity at the unusual C4 site in SMCC reactions of 2,4-dibromopyridine, consistent with Fairlamb's studies using the $[Pd_3(\mu\text{-Cl})(\mu\text{-PPh}_2)_2(PPh_3)_3]^+X^-$ cluster and low $PPh_3/Pd(OAc)_2$ ratios (*vide supra*).[38] Under the cross-coupling conditions, stabilization of the degradation product by the salts present may lead to convergence on a common active species, resulting in the observed atypical selectivity. The findings around **XIV** constitute a rare example of a phosphine-stabilized Pd_3 cluster formed en route to PdNPs (being fully structurally characterized) and validated as an active catalytic species in its own right. Similarly to the historical literature on $[Pd_3(\mu\text{-Cl})(\mu\text{-PPh}_2)_2(PPh_3)_3]^+X^-$, **XIV** has appeared in the coordination chemistry literature before. It forms on reduction of the dicationic complex $[Pd^{II}(\mu\text{-OH})(PPh_3)_2][BF_4]_2$ (note: formed in the presence of Ag^I),[92] where ethanol (solvent) and PPh_3 were identified as dual reductants (acetaldehyde and O═PPh_3 being byproducts). The linear Pd_3 cluster **XIV** can also be generated from the reaction of *trans*-$[Pd(OAc)_2(PPh_3)_2]$ (formed by reacting $Pd(OAc)_2$ with 2 equiv of PPh_3; *vide supra*) with excess triflic acid, with the methanol solvent as a potential reductant.[93] The two Pd−Pd-bonded species $[Pd^I_2(OTf)_2(PPh_3)_2]$ and $[Pd_3(OTf)_2(PPh_3)_2]$—similarly stabilized by π-Ar−Pd interactions—were isolated in the solid state from the same reaction solution (note: limited solution characterization data were obtained in this study on these intermediate species). The preliminary catalytic activity of **XIV** and the two isolated intermediates in hydromethoxycarbonylation reactions of alkenes was reported.

Separately, there is evidence that polar solvents such as H_2O, DMF, and DMAc can influence the stability and propagation dynamics of catalytically active species, including PdNPs as a result of their ability to coordinate with Pd.[94] Among these, polar aprotic solvents (e.g., DMF, DMAc, NMP) have been classed as "palladaphilic", due to their ability to activate and stabilize Pd.[80] Obora et al. characterized "ligandless" DMF-stabilized PdNPs (1.0−1.5 nm, measured by TEM), showing high activity (up to 6.0×10^8 {TON}) in Mizoroki−Heck and SMCC reactions using low catalyst loadings (<12 ppm Pd).[95] The PdNPs were straightforwardly synthesized by extended heating of a DMF solution of $PdCl_2$, in the absence of any additional additives. Analogous DMF-stabilized PdNPs derived from $Pd(OAc)_2$ demonstrated catalytic activity superior to those synthesized from $PdCl_2$ in SMCC applications.[96] Choi et al. employed an LC-MS method to detect small Pd clusters stabilized by DMF (Pd_{10}−Pd_{20}; <3 nm).[97]

H_2O is well-known to play an important role in the formation and stabilization of catalytically active small clusters. Hii et al. delineated a significant, multifaceted role for H_2O in the active speciation of $[Pd_3(OAc)_6]$ in SMCC reactions.[98] The role of such polar solvents in the formation and stabilization of small ligated Pd_n clusters is currently underexplored. Bedford et al. demonstrated that the Pd_3 cluster complex $[Pd_3(OAc)_6]$ could readily hydrolyze on exposure to H_2O, forming a hydroxide-bridged cluster of the form $[Pd_3(\mu\text{-OH})(OAc)_5]$.[99] Fairlamb et al. uncovered a nuanced role for H_2O in catalyst speciation stemming from a *trans*-$[Pd(OAc)_2(N\text{-piperidyl})_2]$ precatalyst in arylcyanation reactions in a highly polar DMAc reaction medium (Figure 12).[12] It was found that the H_2O quantity present had a significant influence on the catalytic performance, with the presence of >4000 ppm of H_2O resulting in a heterogeneous-rooted catalytic manifold involving PdNPs. However, carrying out the reaction under "low-water" conditions (<220 ppm of H_2O) induced a switch to higher activity and a homogeneous catalytic manifold. In the case of the heterogeneous catalytic system formed with excess H_2O (>4000 ppm), H_2O was determined to enable leaching of

https://doi.org/10.1021/acscatal.2c03345
ACS Catal. 2022, 12, 11615−11638

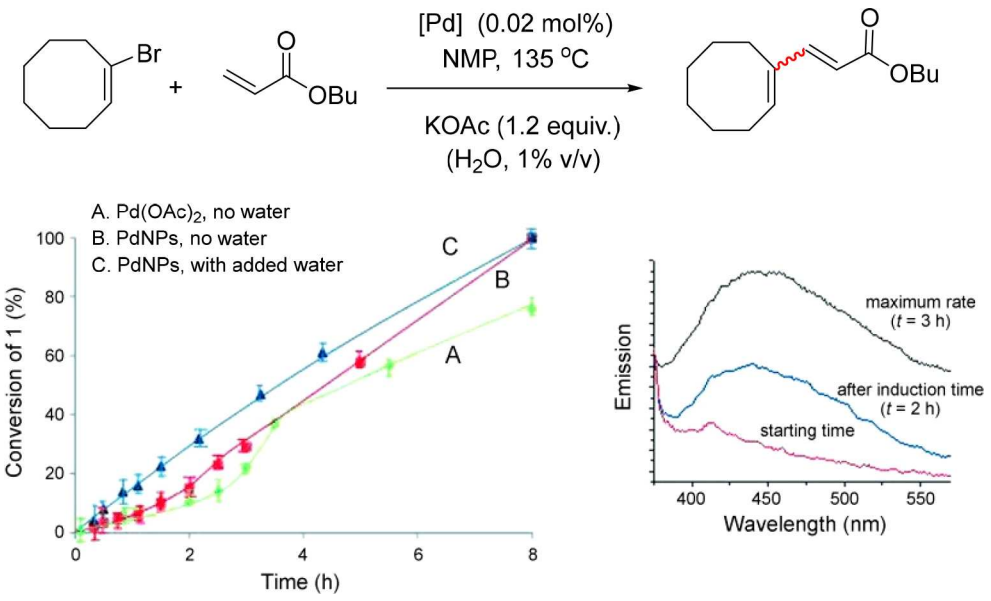

Figure 13. Heck coupling reaction of (*E*)-1-bromocyclooctene with acrylic acid *n*-butyl ester using different palladium catalysts under the employed reaction conditions. (bottom left) Kinetic profile of the reaction with (A) $Pd(OAc)_2$ in the absence of water, (B) Pd nanoparticles in the absence of water, and (C) Pd nanoparticles in the presence of water. (bottom right) Fluorescence spectra for (A) and (B) at different time points. Adapted from ref 14. Copyright 2013 Wiley-VCH.

Scheme 19. Individual Heck, Suzuki, and Sonogashira Cross-Coupling Reactions Catalyzed by either Pt or Pd@EVOH in the Presence of Different Bases, Under the Employed Reaction Conditions

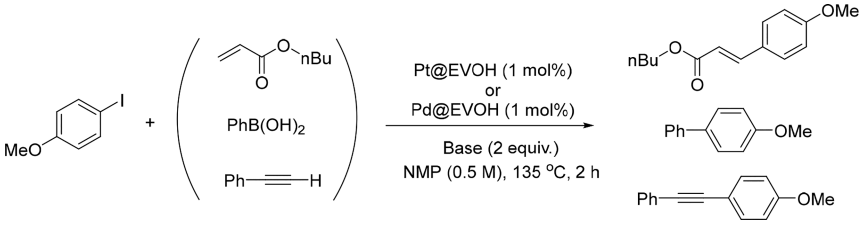

active Pd^0 species from the heterogeneous PdNP source. At <220 ppm of H_2O, a reaction order of 2 in Pd indicated a bimetallic $[Pd^0(L)_n]_2$ (L = N-piperidyl) active species.

Following these studies on the role of H_2O in the speciation of the Pd catalyst, the generation of sub-nanometer Pd_n clusters (n = 3, 4) from the surface of PdNPs stabilized by unhindered nucleophiles, such as H_2O under Heck reaction conditions, was reported by Corma and co-workers.[14] This group reported that the Pd_n clusters (where n = 3, 4) could be dislodged from the surface of PdNPs (ranging from 2.5 to 5.7 nm in diameter) during the Heck coupling of vinyl halides with different olefins. It was found that such species can also be generated after decomposition of other palladium precursors such as $Pd(OAc)_2$, $[Pd_2(dba)_3]$, an oxime-ligated palladacyclic complex, and a $Pd(OAc)_2$/SPhos system under the common Heck reaction conditions. Although the Heck cross-coupling reaction catalyzed by either $Pd(OAc)_2$ or PdNPs (~3.9 nm in diameter) exhibited a sigmoidal kinetic profile under anhydrous reaction conditions, the loss of induction time after addition of H_2O suggested that the contact of H_2O with the surface of palladium nanoparticles instantaneously induces abstraction of Pd_3 and Pd_4 clusters and subsequently increases the overall reaction rate (Figure 13). It was suggested that H_2O acted as a strongly bonded but kinetically labile ligand that enables the displacement of interfering ligands from the coordinating shell of metal atoms on the nanoparticles. These sub-nanometer clusters were characterized by ESI-MS, MALDI-TOF-MS, and UV−vis spectroscopy, although no direct experimental structural evidence was presented for the coordination chemistry of these species. The catalytic systems that were shown to give rise to the clusters also showed substantial catalyst efficacy in Suzuki−Miyaura, Stille, and Sonogashira coupling reactions. It is important to note that Blackmond, Pfaltz et al. revealed that H_2O plays a key role in Heck couplings mediated by palladacycles, particularly in affecting the catalyst induction period.[100]

Corma et al. later reported a series of experimental and computational studies investigating the effect of different bases in the Pd_n- and Pt_n-catalyzed Heck, Suzuki−Miyaura, and Sonogashira cross-couplings of aryl halides under the employed reaction conditions (n < 5).[13] The Pd precatalysts M@EVOH (M = Pd, Pt) were synthesized by dissolution of $Pd(OAc)_2$ or H_2PtCl_4 in a mixture of prepolymeric hydro-alcohol and carvacrol as a reducing agent, followed by extrusion at 80 °C. It was suggested that M@EVOH precatalysts (M = Pd, Pt) liberate small ligand-free Pd_3 and Pt_3 clusters in the reaction media under the employed reaction conditions. The liberation of such clusters within the EVOH material in an isopropanol/water extract was shown by UV−vis absorption spectroscopy, ES-MS, dynamic light scattering (DLS), and high-angle annular dark-field high-resolution transmission electron microscopy (HAADF-HRTEM).

https://doi.org/10.1021/acscatal.2c03345
ACS Catal. 2022, 12, 11615−11638

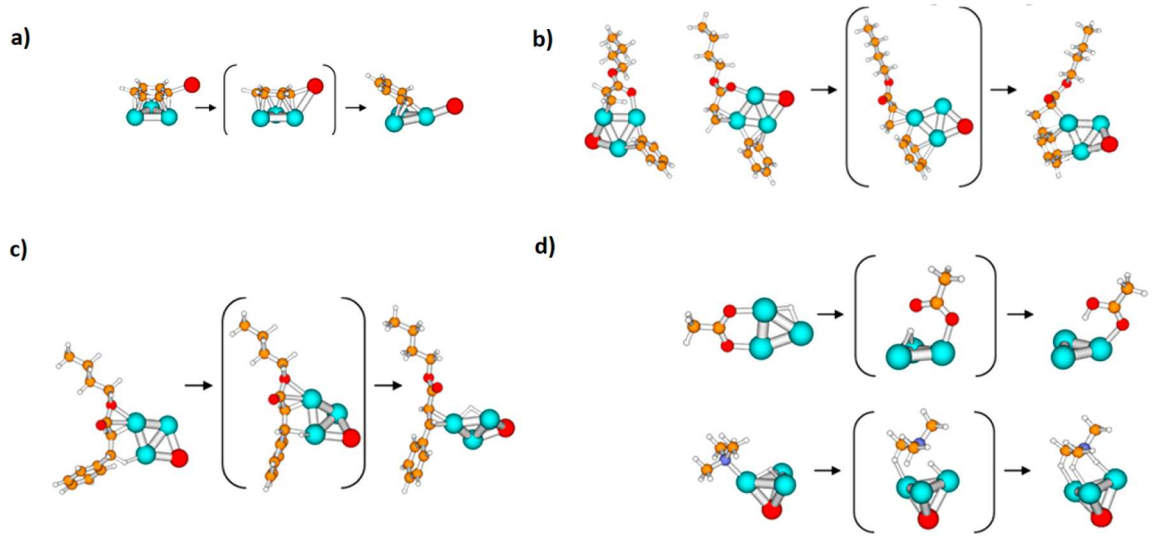

Figure 14. DFT-optimized structures for the oxidative addition of iodobenzene to Pd_3 (a), alkene insertion of iodobenzene into Pd_3 (b), β-elimination step for Pd_3 (c), and reductive elimination step for acetate (d, top) and trimethyl amine as base (d, bottom). Adapted with permission from ref 13. Copyright 2019 American Chemical Society.

Competition reactions showed that sub-nanometer Pd species are active catalysts, where specific bases performed optimally for certain cross-coupling reactions (Scheme 19). Under the conditions examined, the catalyst performance was optimal using amine, carbonate, and phosphate bases for Heck, Sonogashira, and Suzuki−Miyaura cross-coupling reactions, respectively. Aryl chlorides could be activated at more elevated temperatures in NMP (135 °C). Interestingly, for sub-nanometer Pt species, acetate-derived bases were required for good conversion (to products).

The kinetic experiment of Heck coupling of aryl iodides with *n*-butyl acrylate employing precatalytic Pd@EVOH or Pt@EVOH under the reaction conditions showed no visible induction period during the coupling process, suggesting that the release of Pd_n and Pt_n (n = 3, 4) clusters from precatalysts occurs immediately upon initiation of the reaction. Kinetic studies on the Heck reaction of iodobenzene with *n*-butyl acrylate catalyzed by the Pd@EVOH catalyst implicated all reagents, including base, to be involved in the rate-determining step. To further investigate the mechanistic aspects involving the proposed Pd_3 and Pt_3 clusters, DFT calculations were conducted on the four proposed mechanistic steps in a model Heck coupling between iodobenzene and *n*-butyl acrylate. The calculations showed that, in the oxidative addition step, the most stable adsorption of iodobenzene to a Pd_3 cluster was through the arene in an interfacial interaction with the three Pd atoms (Figure 14a).

The difference in the adsorption of aryl halide was justified by the structures of the HOMO and LUMO of both P and Pt clusters, which points to a donation from the HOMO of the Pd cluster to the LUMO of the iodobenzene (σ^* of the C−I bond), as well as a back-bonding from the LUMO of the Pd cluster to the HOMO of the iodobenzene.[13] The activation energies for alkene migratory insertion (Figure 14b) by the coadsorption of *n*-butyl acrylate to the oxidative adducts of Pd_3 species were shown to be high and hence less favored. In this step, it was evident that the carbonyl oxygen atoms from the acrylate could interact with the Pd atoms, playing a stabilizing role. In the β-elimination step, the final most stable isomer of product will be detached from the catalyst species, although the stereospecificity of the product has been derived from *n*-butyl acrylate (similarly to the styrene case) insertion through minimizing the hindrance (Figure 14c). The modeled reductive elimination step involved the regeneration of Pd_3 clusters and release of the coupled product by an interaction involving the base (Figure 14d). This computational work thus supported the notion that the oxidative addition step involving the modeled Pd_3 clusters was not rate-determining, while both the alkene insertion and final reductive elimination steps involving the base were the two more energetically challenging processes for both Pd_3 clusters. This aligned well with the findings reported by Jutand and Amatore, whereby base coordination was found to accelerate reductive elimination involving mononuclear Pd catalysts.[101,102] This work demonstrates that the behavior of small catalytic Pd (and Pt) clusters diverges from their mononuclear Pd species, where oxidative addition or transmetalation is often found to be rate-determining.[103] The differences in reactivity of small Pd_n clusters may allow for future exploitation in challenging and/or site-selective transformations.

It can be argued that the characterization of sub-nanometer Pd_3 and Pt_3 clusters requires more sensitive techniques such as extended X-ray absorption fine structure (EXAFS) and X-ray absorption near-edge structure (XANES) to study the reactions at a molecular level and gain structural information on the active catalytic species. The acquisition of these data can provide evidence of the changes occurring in the Pd coordination environment and possible geometry of the Pd_n clusters during the catalysis (*in operando*). Such data are critical for an experimental validation of theoretical predictions: i.e., ensuring that the Pd_n cluster species detected are indeed catalytically relevant.

3. CHEMICAL BONDING PROPERTIES OF Pd_n CLUSTERS AND THEIR ELECTRONIC EFFECTS ON CATALYSIS

To explore the catalytic reactivity of Pd_n clusters, with a view to understanding how to control and enhance reactivity and product selectivity in transition-metal-catalyzed transformations, it is prudent to examine the electronic properties of Pd_n

https://doi.org/10.1021/acscatal.2c03345
ACS Catal. 2022, 12, 11615−11638

clusters. A detailed understanding of the bonding character within well-defined, ligated Pd_n clusters may allow for the fine-tuning of the catalytic behavior.

After an initial synthesis of the triangular Pd_3 cluster by Coulson et al., Dixon et al. fully characterized $[Pd_3(\mu\text{-}Cl)(\mu\text{-}PPh_2)_2(PPh_3)_3]^+[BF_4]^-$. The X-ray diffraction structure determined from a single crystal showed Pd−Pd interactions at lengths less than that of the sum of the van der Waals radius (2.89 Å for the distance bridged by halogen and 2.93 pm for the other two distances).[17,19,104] A theoretical study by Li et al.[105] on a related analogue of this Pd_3 cluster, which has not yet been reported as an isolable entity, namely $[Pd_3X_3(PH_3)_3]^+$ (X = F^-, Cl^-, Br^-, I^-), revealed that the catalytic properties of trinuclear Pd_3 clusters can be influenced by tuning the chemical bonding interactions between the metal and ligands, demonstrated by computational calculations (using DFT methods; note that PH_3 was used as an electronic model for PPh_3, thereby negating the steric effects of this ligand). An increase in the interatomic distance between Pd−Pd and Pd−X was observed as the bridging halide anion was altered from fluoride to chloride, bromide, and iodide, which was reasoned by an increasing ionic radius and subsequent reduction in the Pd−Pd bond strength. An investigation into the electronic structure of the Pd_3 cluster showed that the HOMO was mainly formed from $\pi(Pd_3^{4+})$ and $\pi_v^*(X_3^{3-})$ fragments. However, the LUMO derives from the σ^* orbital of Pd_3 and PH_3 fragments, indicating that four d electrons of the Pd_3 triangle are oxidized to form a stable Pd_3^{4+} cluster core; hence. the formal oxidation state of the Pd_3 cluster is +4 (+4/3 per Pd). The key message from this study is that the HOMO is substantially affected by different halogen-bridging ligands and LUMOs by the PH_3 terminal ligands. As a result, the HOMO−LUMO energy gap decreases as the halogen changes in the order Cl > Br > I in the group, with $[Pd_3Cl_3(PH_3)_3]^+$ having the largest HOMO−LUMO gap and hence the most stable structure (Figure 15).

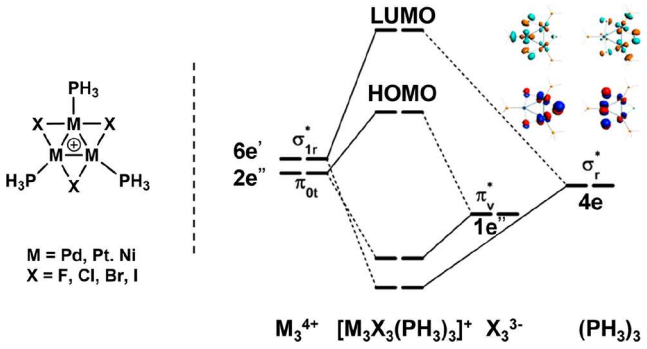

Figure 15. Simplified orbital energy correlation diagram of $[M_3X_3(PH_3)_3]^+$ (M = Pd, Pt, Ni and X = F, Cl, Br, I). Adapted with permission from ref 105. Copyright 2017 American Chemical Society.

Energy decomposition analysis with natural orbitals for chemical valency (EDA-NOCV) calculations, which examined the interactions between Pd and both bridging and terminal ligand orbitals, displayed two degenerate contributions implying σ-donation from both bridging ligands and terminal ligands toward the Pd_3^{4+} core and a weak σ-back-donation from the cationic Pd_3 core toward the ligands. It was determined that the charge flow in this channel increases with heavier halogen ligands. Moreover, the electron pairs are also localized at the Pd_3 center, which implies three-center−two-electron bonding and metallic aromaticity within the trinuclear Pd_3 clusters, a hypothesis supported by nucleus-independent chemical shift (NICS) values and electron localization function (ELF) plots. Such all-metal aromaticity was described, along with experimental evidence in the analogous C_3-symmetric $[Pd_3(\mu\text{-}SAr')(PAr_3)_3]^+X^-$ cluster complexes, as reported by Maestri and Malacria.[55] The catalytic properties of the Pd_3 clusters in the simple adsorption of H_2 was computationally investigated by the same team. The results highlight the distinct effect of varying the bridging halogen ligands on the shape of the cluster and the bond strength of Pd−X (X= F, Cl, Br, I). The insertion of H_2 into the Pd_3 cluster structure triggers a site activation of the Pd−X bond and subsequently a potential substitution of bridging halogen by other incoming molecules (Figure 16).

In another study on triangular Pd_3 structures, Malacria and Mastri et al. reported the synthesis of C_3-symmetric 44-core-valence-electron cluster $[Pd_3(\mu\text{-}SAr')(PAr_3)_3]^+$, with an equilateral triangular core that shares similarities with Lewis acids.[53] A computational study (using DFT methods) confirmed that all three Pd atoms were almost equivalent and their chemical bonding features a fully delocalized three-center−two-electron bonding arrangement, analogous to the organic aromatic cyclopropenium systems. On the other hand, a nucleus-independent chemical shift (NICS) analysis also produced large negative values for the cationic Pd_3 cluster that are likely to occur for electron-rich, neutral, or anionic species. This suggests that the cationic Pd_3 clusters also possess electron-rich bonding properties that enable them to act as a Lewis base. Indeed, the investigation examined possible interactions of the delocalized Pd_3 planar core in the clusters with cations such as Li^+ and group XI M(I) species (M = Cu, Ag, Au), either through noncovalent bonding or via coordination.[56] The calculated binding energy for these cations to the Pd_3 core showed a large negative ΔG contribution, with concomitant formation of a metal-edged tetrahedral cap of the $[Pd_3]^+$ cluster. Novel dicationic $[Pd_3M]^{2+}$ clusters were thus synthesized and successfully crystallized (stabilizing anion SbF_6^- or BF_4^-). The X-ray crystal structure of a $[Pd_3Ag]^{2+}$ species (Figure 17) shows that the Ag atom lies 2.4 Å above the center of the planar $[Pd_3]^+$ triangle core, where the Ag atom is ligated by three molecules of H_2O. The Pd−Pd distances were found to be close to those in its unbound state. Furthermore, the P and S atoms of the $[Pd_3Ag]^{2+}$ triangle remain coplanar with the Pd_3 triangle.

The modeling of the $[Pd_3M]^{2+}$ clusters represented only HOMO bonding orbitals for the four metal nuclei; the other MOs including LUMOs were essentially unaffected by the interaction with a different metals. This correlates with a minimal structural reorganization occurring from $[Pd_3]^+$ to $[Pd_3M]^{2+}$ (M = Cu, Ag, Au).

A computational investigation with $[Pd_3(\mu\text{-}X)(\mu\text{-}PPh_2)_2(PPh_3)_3]^+$ (shortened here as $\mathbf{Pd_3{\cdot}X}$) carried out by Li et al. showed that these clusters possess large HOMO−LUMO energy gaps of 2.61, 2.55, and 2.19 eV for X = Cl, Br, Ph, respectively, accounting for their high stability under aerobic conditions (Figure 18).[19] A computational study on the simplified model cluster $[Pd_3(PH_2)_3(PH_3)_3]^+Cl^-$ exhibited square d(sp^2) hybridization of Pd, which accounted for the planarity of these clusters along with a three-center−two-electron Pd−Pd−Pd triangle. The bridging ligands were suggested to result in stability for triangular Pd_3 within the

https://doi.org/10.1021/acscatal.2c03345
ACS Catal. 2022, 12, 11615−11638

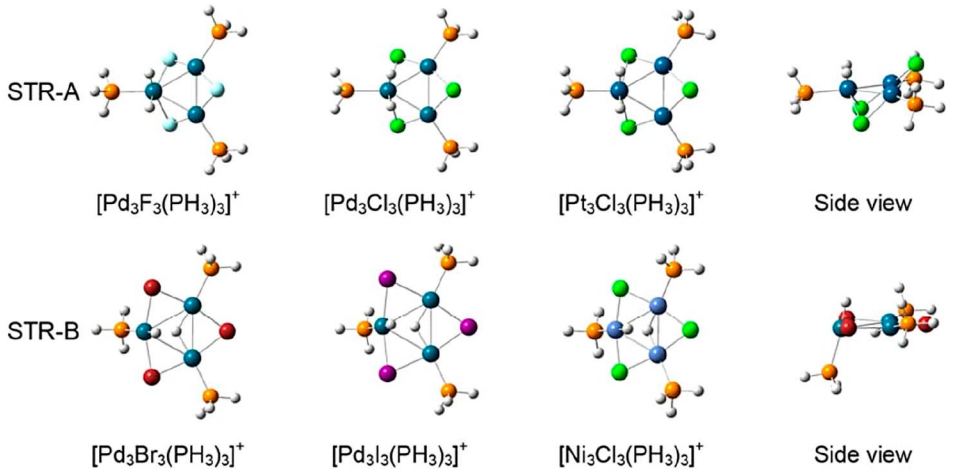

Figure 16. Structures of $H_2@[Pd_3X_3(PH_3)_3]^+$ (X = F, Cl, Br, I), H2@$[Pt_3Cl_3(PH_3)_3]^+$, and H2@$[Ni_3Cl_3(PH_3)_3]^+$ clusters. Two types of adsorption structures are found and denoted as STR-A and STR-B. Adapted with permission from ref 105. Copyright 2017 American Chemical Society.

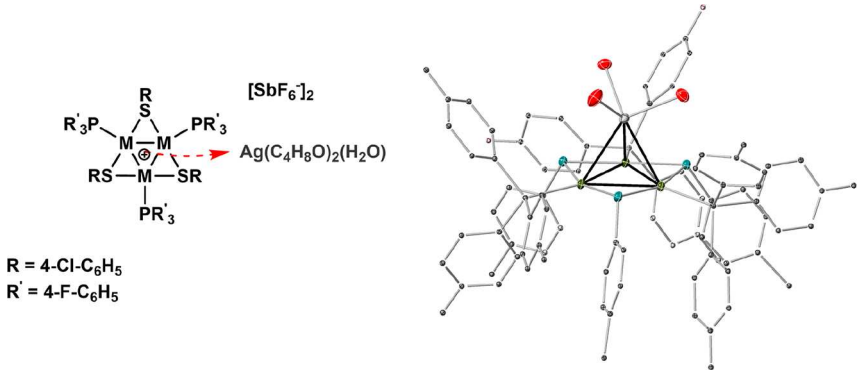

Figure 17. Crystal structure of the $[Pd_3Ag]^{2+}$ complex (reprocessed in CrystalMaker X). Thermal ellipsoids are shown at 15% probability, H atoms and solvent of crystallization are not shown, for clarity. The dashed red arrow depicts coordination of the cationic Pd_3 entity to Ag (only oxygen atoms of the Ag fragment are shown for clarity). Bond lengths (Å) and angles (deg) for the $[Pd_3Ag]^{2+}$ complex: Ag− Pd(1) = 2.8530 (10); Ag− Pd(2) = 2.8092 (10); Ag− Pd(2) = 2.824; Pd(1)−Ag−Pd(3) = 61.414. Adapted from ref 56. Licensed under Creative Commons.

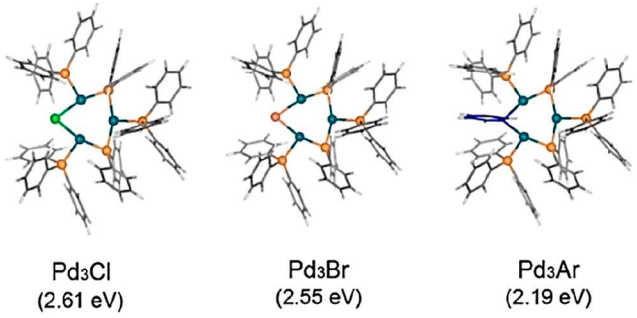

Figure 18. Optimized structures of $[Pd_3(\mu\text{-X})(\mu\text{-PPh}_2)_3(PPh_3)_3]^+$ (X = Cl, Br, Ar) denoted as Pd_3Cl, Pd_3Br, and Pd_3Ar, respectively (the calculated HOMO−LUMO energy gaps are indicated in parentheses at the bottom of their structures). Adapted with permission from ref 19. Copyright 2017 American Chemical Society.

cluster. Likewise, for **Pd_3Cl**, it was suggested that the bulk hindrance provided by bridging PPh_2 and terminal PPh_3 ligands makes the approach of substrates to the triangular core in $[Pd_3(\mu\text{-Cl})(\mu\text{-PPh}_2)_2(PPh_3)_3]^+$ difficult, protecting the Pd cluster from possible decomposition during catalyst turnover. The HOMO−LUMO energy gaps determined by DFT methods for $[Pd_3(\mu\text{-Cl})(\mu\text{-PPh}_2)_2(PPh_3)_3]^+$, $[Pd_3(\mu\text{-Br})(\mu\text{-PPh}_2)_2(PPh_3)_3]^+$, and $[Pd_3(\mu\text{-Ar})(\mu\text{-PPh}_2)_2(PPh_3)_3]^+$ clusters show that the HOMO−LUMO energy gap is lower; the authors pointed to these species being less stable than the halide derivatives (the absolute energy values for the HOMO and LUMO of these species were not reported in the paper). We have been unable to examine the structures more closely due to the output files not being available in the original publication.[19]

The reactivity of $[Pd_3(\mu\text{-Cl})(\mu\text{-PPh}_2)_2(PPh_3)_3]^+$ was examined by exposure to the partially soluble base K_2CO_3 in "aqueous solvent", without any substrates being present, leading to the formation of $[Pd_3(\mu\text{-OH})(\mu\text{-PPh}_2)_2(PPh_3)_3]^+$ species resulting from the substitution of bridging chloride by hydroxide (note: from the original paper it appears that CH_2Cl_2 was used). The study suggested that the μ-Cl can act as an active site when it is exposed to an appropriate nucleophile and base. On the other hand, the study by Malacria et al.[102] showed that the cationic Pd_3 triangular core could be an active site for incoming electrophiles. This duality in reactivity is unique to Pd_3 clusters of this type and could potentially be exploited more widely in chemical synthesis.

https://doi.org/10.1021/acscatal.2c03345
ACS Catal. 2022, 12, 11615−11638

4. CONCLUDING REMARKS AND FUTURE PERSPECTIVES

The catalytic applications and chemical bonding properties of Pd_n clusters have been examined in this review. It is envisioned that this compiled information can enable researchers to understand the factors that may lead to manipulation of catalytic activity by modulation of the structure, with the primary aim of improving catalytic efficacy and performance. Small, well-defined Pd_n clusters have been shown to form through the transformation of dinuclear (Pd_2) to trinuclear (Pd_3) clusters of related structures,[17,23] generated from the combination of Pd^0 or Pd^{II} monomeric species, or by leaching from a PdNP surface[4,13] in the reaction media, in the form of both ligand-free or ligand-stabilized systems (with phosphine ligands, for example). Moreover, studies focused on the catalytic reactivity and selectivity of Pd_3 clusters in SMCC reactions and hydrogenation reactions showed that the structure of Pd_n clusters can remain intact throughout the lifetime of a catalytic process. Taken together, the combination of these findings demonstrates that higher-order Pd_n species are catalytically active under specific reaction conditions and therefore perform as one of the catalyst species, potentially alongside other "cocktails" of the catalytic species occurring in a reaction mixture.[76]

Having collated research papers in this area, it is pertinent to mention the techniques required to characterize Pd_n cluster catalysis. In addition to conventional techniques (such as IR, UV−vis, NMR, MS, single-crystal XRD), one can employ kinetic studies to analyze the catalytic behavior of the reaction system under investigation—an example being reported by Fairlamb et al.[12] Other techniques such as X-ray absorption spectroscopy (XANES/EXAFS) could be useful for characterizing species under working reaction conditions. Fluorescence measurements are emerging as a useful tool for probing the homogeneous−heterogeneous catalysis question. We believe that is critical that any Pd_n cluster species proposed is supported by at least two independent methods of characterization. Furthermore, raw data from XANES/EXAFS measurements should be made available to others to confirm modeling and characterization. Computational methods are important in the characterization of Pd_n clusters, although there are limitations with larger systems, particularly where there are labile or flexible ligands (e.g., PPh_3). From a catalysis perspective we have reservations (for DFT studies) about employing PH_3 as a model ligand for PPh_3 in these complicated Pd_n cluster systems.

On the basis of the global findings regarding the structure of Pd_n clusters, and associated catalytic activities, we are confident that multinuclear Pd clusters can serve as a framework for novel catalyst design. With efficiency, atom economy, selectivity, and reactivity of cross-coupling catalyst system in mind, Pd_n clusters are viable alternatives for traditional $Pd^0(L)_n$ or small-size PdNPs as active catalysts. A deeper understanding and control of the dynamics of formation and propagation of Pd_n clusters may allow access to unique catalytic activity and downstream chemical space. Finally, pathways involving Pd_n clusters should be considered when delineating the mechanisms of novel cross-coupling processes involving Pd catalyst species.

AUTHOR INFORMATION

Corresponding Author

Ian J. S. Fairlamb − *Department of Chemistry, University of York, York, North Yorkshire, U.K. YO10 5DD*; orcid.org/0000-0002-7555-2761; Email: ian.fairlamb@york.ac.uk

Authors

Neda Jeddi − *Department of Chemistry, University of York, York, North Yorkshire, U.K. YO10 5DD*

Neil W. J. Scott − *Department of Chemistry, University of York, York, North Yorkshire, U.K. YO10 5DD*; orcid.org/0000-0002-6613-148X

Complete contact information is available at: https://pubs.acs.org/10.1021/acscatal.2c03345

Author Contributions

N.J. and N.W.J.S. contributed equally to the writing of this review.

Notes

The authors declare no competing financial interest.

ABBREVIATIONS

Dba, (*E*,*E*)-dibenzylidene acetone
DFT, density functional theory
DLS, dynamic light scattering
EDA-NOCV, energy decomposition analysis with natural orbitals for chemical valency
ELF, electron localization function
ESI-TOF, electrospray ionization with time-of-flight mass spectroscopy
EXAFS, extended X-ray absorption fine structure
HAADF-HRTEM, high-angle annular dark-field high-resolution transmission electron microscopy
HOMO, highest occupied molecular orbital
LUMO, lowest unoccupied molecular orbital
MALDI-MS, matrix-assisted laser desorption/ionization
MOF, metal−organic framework
MSI, metal−support interaction
NICS, nucleus-independent chemical shift
OTf, triflate (trifluoromethylsulfonate ($-OS(O)_2CF_3$))
Pd_3X·X, $[Pd_3(\mu\text{-}SR)_2(\mu\text{-}PPh_2)_2(PPh_3)_3]$, X = halide
SET, single-electron transfer
SMCC, Suzuki−Miyaura cross-coupling reaction
SPhos, 2-dicyclohexylphosphino-2′,6′-dimethoxybiphenyl
TEM, transmission electron microscopy
TiNT, titania nanotube
TON, catalyst turnover number
TOF, catalyst turnover frequency
TPSSh, Tao, Perdew, Staroverov, and Scuseria
Tr, cycloheptatrienyl ligand
XANES, X-ray absorption near-edge structure
XRD, X-ray diffraction

REFERENCES

(1) Wu, X.-F.; Anbarasan, P.; Neumann, H.; Beller, M. From noble metal to Nobel Prize: palladium-catalyzed coupling reactions as key methods in organic synthesis. *Angew. Chem., Int. Ed.* **2010**, *49*, 9047−9050.

(2) De Ornellas, S.; Williams, T. J.; Baumann, C. G.; Fairlamb, I. J. S. In *C-H and C-X Bond Functionalization: Transition Metal Mediation*; RSC Publishing: 2013; pp 409−447.

(3) Ingoglia, B. T.; Wagen, C. C.; Buchwald, S. L. Biaryl monophosphine ligands in palladium-catalyzed C−N coupling: An updated User's guide. *Tetrahedron* **2019**, *75*, 4199−4211.
(4) Polynski, M. V.; Ananikov, V. P. Modeling Key Pathways Proposed for the Formation and Evolution of "Cocktail"-Type Systems in Pd-Catalyzed Reactions Involving ArX Reagents. *ACS Catal.* **2019**, *9*, 3991−4005.
(5) Eremin, D. B.; Ananikov, V. P. Understanding active species in catalytic transformations: From molecular catalysis to nanoparticles, leaching,"Cocktails" of catalysts and dynamic systems. *Coord. Chem. Rev.* **2017**, *346*, 2−19.
(6) Fricke, C.; Sperger, T.; Mendel, M.; Schoenebeck, F. Catalysis with Palladium(I) Dimers. *Angew. Chem., Int. Ed.* **2021**, *60*, 3355−3366.
(7) Amatore, C.; Jutand, A.; M'Barki, M. A. Evidence of the Formation of Zerovalent Palladium from $Pd(OAc)_2$, and Triphenylphosphine. *Organometallics* **1992**, *11*, 3009−3013.
(8) Fors, B. P.; Krattiger, P.; Strieter, E.; Buchwald, S. L. Water-Mediated Catalyst Preactivation: An Efficient Protocol for C−N Cross-Coupling Reactions. *Org. Lett.* **2008**, *10*, 3505−3508.
(9) Amatore, C.; El Kaïm, L.; Grimaud, L.; Jutand, A.; Meignié, A.; Romanov, G. Kinetic Data on the Synergetic Role of Amines and Water in the Reduction of Phosphine-Ligated Palladium(II) to Palladium(0). *Eur. J. Org. Chem.* **2014**, *2014*, 4709−4713.
(10) Shaughnessy, K. H. Development of Palladium Precatalysts that Efficiently Generate LPd(0) Active Species. *Isr. J. of Chem.* **2020**, *60*, 180−194.
(11) (a) Ellis, P. J.; Fairlamb, I. J. S.; Hackett, S. F. J.; Wilson, K.; Lee, A. F. Evidence for the Surface-Catalyzed Suzuki−Miyaura Reaction over Palladium Nanoparticles: An Operando XAS Study. *Angew. Chem., Int. Ed.* **2010**, *49*, 1820−1824. (b) Lee, A. F.; Ellis, P. J.; Fairlamb, I. J. S.; Wilson, K. *Dalton Trans.* **2010**, *39*, 10473−10482.
(12) Bray, J. T. W.; Ford, M. J.; Karadakov, P. B.; Whitwood, A. C.; Fairlamb, I. J. S. The critical role played by water in controlling Pd catalyst speciation in arylcyanation reactions. *React. Chem. Eng.* **2019**, *4*, 122−130.
(13) Fernández, E. a.; Rivero-Crespo, M. A.; Domínguez, I.; Rubio-Marqués, P.; Oliver-Meseguer, J.; Liu, L.; Cabrero-Antonino, M. a.; Gavara, R.; Hernández-Garrido, J. C.; Boronat, M.; Leyva-Pérez, A.; Corma, A. Base-controlled Heck, Suzuki, and Sonogashira reactions catalyzed by ligand-free platinum or palladium single atom and sub-nanometer clusters. *J. Am. Chem. Soc.* **2019**, *141*, 1928−1940.
(14) Leyva-Pérez, A.; Oliver-Meseguer, J.; Rubio-Marqués, P.; Corma, A. Water-Stabilized Three-and Four-Atom Palladium Clusters as Highly Active Catalytic Species in Ligand-Free C−C Cross-Coupling Reactions. *Angew. Chem., Int. Ed.* **2013**, *52*, 11554−11559.
(15) Burrows, A. D.; Mingos, D. M. P. The chemistry of group 10 metal triangulo clusters. *Coord. Chem. Rev.* **1996**, *154*, 19−69.
(16) Burrows, A. D.; Michael, D.; Mingos, P. Palladium cluster compounds. *Transition Met. Chem.* **1993**, *18*, 129−148.
(17) Scott, N. W.; Ford, M. J.; Schotes, C.; Parker, R. R.; Whitwood, A. C.; Fairlamb, I. J. The ubiquitous cross-coupling catalyst system 'Pd (OAc) 2'/2PPh 3 forms a unique dinuclear Pd I complex: an important entry point into catalytically competent cyclic Pd 3 clusters. *Chem. Sci.* **2019**, *10*, 7898−7906.
(18) Johansson Seechurn, C. C. C.; Sperger, T.; Scrase, T. G.; Schoenebeck, F.; Colacot, T. J. Understanding the Unusual Reduction Mechanism of Pd(II) to Pd(I): Uncovering Hidden Species and Implications in Catalytic Cross-Coupling Reactions. *J. Am. Chem. Soc.* **2017**, *139*, 5194−5200.
(19) Fu, F.; Xiang, J.; Cheng, H.; Cheng, L.; Chong, H.; Wang, S.; Li, P.; Wei, S.; Zhu, M.; Li, Y. A robust and efficient Pd_3 cluster catalyst for the Suzuki reaction and its odd mechanism. *ACS Catal.* **2017**, *7*, 1860−1867.
(20) Monfredini, A.; Santacroce, V.; Deyris, P.-A.; Maggi, R.; Bigi, F.; Maestri, G.; Malacria, M. Boosting catalyst activity in cis-selective semi-reduction of internal alkynes by tailoring the assembly of all-metal aromatic tri-palladium complexes. *Dalton Trans.* **2016**, *45*, 15786−15790.
(21) Deyris, P. A.; Caneque, T.; Wang, Y.; Retailleau, P.; Bigi, F.; Maggi, R.; Maestri, G.; Malacria, M. Catalytic Semireduction of Internal Alkynes with All-Metal Aromatic Complexes. *ChemCatChem.* **2015**, *7*, 3266−3269.
(22) Lanzi, M.; Cañeque, T.; Marchiò, L.; Maggi, R.; Bigi, F.; Malacria, M.; Maestri, G. Alternative Routes to Tricyclic Cyclohexenes with Trinuclear Palladium Complexes. *ACS Catal.* **2018**, *8*, 144−147.
(23) Diehl, C. J.; Scattolin, T.; Englert, U.; Schoenebeck, F. C− I-Selective Cross-Coupling Enabled by a Cationic Palladium Trimer. *Angew. Chem., Int. Ed.* **2019**, *131*, 217−221.
(24) Mingos, D. M. P.; et al. Synthesis and structural characterisation of $[Pd_2(\mu\text{-}Br)_2(PtBu_3)_2]$, an example of a palladium (I)−palladium (I) dimer. *J. Chem. Soc., Dalton Trans.* **1996**, 4313−4314.
(25) Durà-Vilà, V.; Mingos, D. M. P.; Vilar, R.; White, A. J.; Williams, D. J. Reactivity studies of $[Pd2\ (\mu\text{-}X)_2(PtBu_3)_2](X = Br, I)$ with CNR (R= 2, 6-dimethylphenyl), H_2 and alkynes. *J. Organomet. Chem.* **2000**, *600*, 198−205.
(26) Durà-Vilà, V.; Mingos, D. M. P.; Vilar, R.; White, A. J.; Williams, D. J. Insertion of O2 into a Pd (I)−Pd (I) dimer and subsequent C−O bond formation by activation of a C−H bond. *Chem. Commun.* **2000**, 1525−1526.
(27) Stambuli, J. P.; Kuwano, R.; Hartwig, J. F. Unparalleled rates for the activation of aryl chlorides and bromides: Coupling with amines and boronic acids in minutes at room temperature. *Angew. Chem., Int. Ed.* **2002**, *41*, 4746−4748.
(28) Lin, W.; Wilson, S. R.; Girolami, G. S. Synthesis and X-ray Crystal Structure of the New Palladium(I) Dimer $[Pd_2(PMe_3)_6]$-$[hfac]_2$ and Its Conversion to $[PdMe(PMe_3)_3][hfac]$ via Activation of Phosphorus-Carbon Bonds. *Inorg. Chem.* **1994**, *33*, 2265−2272.
(29) Proutiere, F.; Schoenebeck, F. Solvent Effect on Palladium-Catalyzed Cross-Coupling Reactions and Implications on the Active Catalytic Species. *Angew. Chem., Int. Ed.* **2011**, *50*, 8192−8195.
(30) Bonney, K. J.; Proutiere, F.; Schoenebeck, F. Dinuclear Pd (I) complexes—solely precatalysts? Demonstration of direct reactivity of a Pd (I) dimer with an aryl iodide. *Chem. Sci.* **2013**, *4*, 4434−4439.
(31) Legault, C. Y.; Garcia, Y.; Merlic, C. A.; Houk, K. N. Origin of regioselectivity in palladium-catalyzed cross-coupling reactions of polyhalogenated heterocycles. *J. Am. Chem. Soc.* **2007**, *129*, 12664−12665.
(32) Labios, L. A.; Millard, M. D.; Rheingold, A. L.; Figueroa, J. S. Bond activation, substrate addition and catalysis by an isolable two-coordinate Pd(0) bis-isocyanide monomer. *J. Am. Chem. Soc.* **2009**, *131*, 11318−11319.
(33) Barnett, B. R.; Labios, L. A.; Stauber, J. M.; Moore, C. E.; Rheingold, A. L.; Figueroa, J. S. Synthetic and Mechanistic Interrogation of Pd/Isocyanide-Catalyzed Cross-Coupling: π-Acidic Ligands Enable Self-Aggregating Monoligated Pd(0) Intermediates. *Organometallics* **2017**, *36*, 944−954.
(34) Arif, A. M.; Heaton, D. E.; Jones, R. A.; Nunn, C. M. Di- and trinuclear di-tert-butylphosphido-bridged complexes of palladium. Synthesis and x-ray structures of $[Pd(\mu\text{-tert-}Bu_2P)(PMe_3)]_2$(Pd-Pd) and mixed-valence $Pd_3(\mu\text{-tert-Bu2P})(CO)_2Cl$. *Inorg. Chem.* **1987**, *26*, 4228−4231.
(35) Amatore, C.; Carre, E.; Jutand, A.; M'Barki, M. A.; Meyer, G. Evidence for the Ligation of Palladium(0) Complexes by Acetate Ions: Consequences on the Mechanism of Their Oxidative Addition with Phenyl Iodide and PhPd(OAc)(PPh3)2 as Intermediate in the Heck Reaction. *Organometallics* **1995**, *14*, 5605−5614.
(36) Amatore, C.; Carre, E.; Jutand, A.; M'Barki, M. A. Rates and Mechanism of the Formation of Zerovalent Palladium Complexes from Mixtures of Pd(OAc)2 and Tertiary Phosphines and Their Reactivity in Oxidative Additions. *Organometallics* **1995**, *14*, 1818−1826.
(37) Polymorphic form of "$Pd(OAc)_2$" (e.g., $Pd_3(OAc)_6$ or its polymeric form) not specified.
(38) Scott, N. W. J.; Ford, M. J.; Jeddi, N.; Eyles, A.; Simon, L.; Whitwood, A. C.; Tanner, T.; Willans, C. E.; Fairlamb, I. J. S. A Dichotomy in Cross-Coupling Site Selectivity in a Dihalogenated

https://doi.org/10.1021/acscatal.2c03345
ACS Catal. 2022, 12, 11615−11638

Heteroarene: Influence of Mononuclear Pd, Pd Clusters, and Pd Nanoparticles—the Case for Exploiting Pd Catalyst Speciation. *J. Am. Chem. Soc.* **2021**, *143*, 9682−9693.
(39) Wagschal, S.; Perego, L. A.; Simon, A.; Franco-Espejo, A.; Tocqueville, C.; Albaneze-Walker, J.; Jutand, A.; Grimaud, L. Formation of XPhos-Ligated Palladium(0) Complexes and Reactivity in Oxidative Additions. *Chem. - Eur. J.* **2019**, *25*, 6980−6987.
(40) Montgomery, M.; O'Brien, H. M.; Méndez-Gálvez, C.; Bromfield, C. R.; Roberts, J. P.; Winnicka, A. M.; Horner, A.; Elorriaga, D.; Sparkes, H. A.; Bedford, R. B. The surprisingly facile formation of Pd (I)−phosphido complexes from ortho-biphenylphosphines and palladium acetate. *Dalton Trans.* **2019**, *48*, 3539−3542.
(41) Scott, N. W. J.; Ford, M. J.; Husbands, D. R.; Whitwood, A. C.; Fairlamb, I. J. S. Reactivity of a Dinuclear PdI Complex $[Pd_2(\mu\text{-}PPh_2)(\mu_2\text{-}OAc)(PPh_3)_2]$ with PPh_3: Implications for Cross-Coupling Catalysis Using the Ubiquitous $Pd(OAc)_2/nPPh_3$ Catalyst System. *Organometallics* **2021**, *40*, 2995−3002.
(42) Amatore, C.; Jutand, A.; Meyer, G. Unexpected bell-shaped effect of the ligand on the rate of the oxidative addition to palladium(0) complexes generated in situ from mixtures of $Pd(dba)_2$ and para-substituted triarylphosphines. *Inorg. Chim. Acta* **1998**, *273*, 76−84.
(43) Macé, Y.; Kapdi, A. R.; Fairlamb, I. J. S.; Jutand, A. Influence of the dba Substitution on the Reactivity of Palladium(0) Complexes Generated from $Pd^0{}_2(dba\text{-}n,n'\text{-}Z)_3$ or $Pd^0(dba\text{-}n,n'\text{-}Z)_2$ and PPh_3 in Oxidative Addition with Iodobenzene. *Organometallics* **2006**, *25*, 1795−1800.
(44) Sicre, C.; Alonso-Gómez, J. L.; Cid, M. M. Regioselectivity in alkenyl(aryl)-heteroaryl Suzuki cross-coupling reactions of 2,4-dibromopyridine. A synthetic and mechanistic study. *Tetrahedron* **2006**, *62*, 11063−11072.
(45) Cassol, C. C.; Umpierre, A. P.; Machado, G.; Wolke, S. I.; Dupont, J. The Role of Pd Nanoparticles in Ionic Liquid in the Heck Reaction. *J. Am. Chem. Soc.* **2005**, *127*, 3298−3299.
(46) Chernyshev, V. M.; Khazipov, O. V.; Eremin, D. B.; Denisova, E. A.; Ananikov, V. P. Formation and stabilization of nanosized Pd particles in catalytic systems: Ionic nitrogen compounds as catalytic promoters and stabilizers of nanoparticles. *Coord. Chem. Rev.* **2021**, *437*, 213860.
(47) Coulson, D. R. Ready cleavage of triphenylphosphine. *Chem. Commun. (London)* **1968**, 1530−1531.
(48) Bushnell, G. W.; Dixon, K. R.; Moroney, P.; Rattray, A. D.; Ch'eng, W. Synthesis and 31P Nuclear Magnetic Resonance Studies of Trinuclear Palladium Cluster Complexes X-Ray Structure of [Pd, Cl(PPh,), (PEt,),] [BF4]. *J. Chem. Soc., Chem. Commun.* **1977**, 709−710.
(49) Berry, D. E.; Bushnell, G. W.; Dixon, K. R.; Moroney, P. M.; Wan, C. e. Palladium clusters. 4. Synthesis and ^{31}P and ^{195}Pt NMR study of a mixed platinum/palladium cation, $[PtPd_2Cl(PPh_2)_2(PPh_3)_3]+$, and the crystal and molecular structures of $[Pd_3Cl(PPh_2)_2(PEt_3)_3][BF_4]$, $[Pd_3Cl(PPh_2)_2(PPh_3)_3][BF_4]$, and $[Pt_{0.81}Pd_{2.19}Cl(PPh_2)_2(PPh_3)_3][BF_4]$. *Inorg. Chem.* **1985**, *24*, 2625−2634.
(50) Berenblyum, A. S.; Aeeva, A. P.; Lakhman, L. I.; Moiseev, I. I. Mechanism of the formation of palladium complexes serving as catalysts in hydrogenation reactions. *J. Organomet. Chem.* **1982**, *234*, 237−248.
(51) Berenblyum, A. S.; Knizhnik, A. G.; Mund, S. L.; Moiseev, I. I. Mechanism of the formation of palladium complexes serving as catalysts in hydrogenation reactions. *J. Organomet. Chem.* **1982**, *234*, 219−235.
(52) Moiseev, I. I.; Vargaftik, M. N. Pd cluster catalysis: a review of reactions under anaerobic conditions. *New J. Chem.* **1998**, *22*, 1217−1227.
(53) Blanchard, S.; Fensterbank, L.; Gontard, G.; Lacôte, E.; Maestri, G.; Malacria, M. Synthesis of triangular tripalladium cations as noble-metal analogues of the cyclopropenyl cation. *Angew. Chem., Int. Ed.* **2014**, *53*, 1987−1991.
(54) Bigi, F.; Cera, G.; Maggi, R.; Wang, Y.; Malacria, M.; Maestri, G. Is Aromaticity a Driving Force in Catalytic Cycles? A Case from the Cycloisomerization of Enynes Catalyzed by All-Metal Aromatic Pd_3^+ Clusters and Carboxylic Acids. *J. Phys. Chem. A* **2021**, *125*, 10035−10043.
(55) Wang, Y.; Deyris, P.-A.; Caneque, T.; Blanchard, F.; Li, Y.; Bigi, F.; Maggi, R.; Blanchard, S.; Maestri, G.; Malacria, M. A Simple Synthesis of Triangular All-Metal Aromatics Allowing Access to Isolobal All-Metal Heteroaromatics. *Chem.- Eur. J.* **2015**, *21*, 12271−12274.
(56) Wang, Y.; Monfredini, A.; Deyris, P.-A.; Blanchard, F.; Derat, E.; Maestri, G.; Malacria, M. All-metal aromatic cationic palladium triangles can mimic aromatic donor ligands with Lewis acidic cations. *Chem. Sci.* **2017**, *8*, 7394−7402.
(57) Wang, Y.; Deyris, P. A.; Caneque, T.; Blanchard, F.; Li, Y.; Bigi, F.; Maggi, R.; Blanchard, S.; Maestri, G.; Malacria, M. A Simple Synthesis of Triangular All-Metal Aromatics Allowing Access to Isolobal All-Metal Heteroaromatics. *Chem. - Eur. J.* **2015**, *21*, 12271−12274.
(58) Monfredini, A.; Santacroce, V.; Marchiò, L.; Maggi, R.; Bigi, F.; Maestri, G.; Malacria, M. Semi-Reduction of internal alkynes with prototypical subnanometric metal surfaces: bridging homogeneous and heterogeneous catalysis with trinuclear all-metal aromatics. *ACS Sust. Chem. Eng.* **2017**, *5*, 8205−8212.
(59) Robilotto, T. J.; Bacsa, J.; Gray, T. G.; Sadighi, J. P. Synthesis of a trigold monocation: an isolobal analogue of [H3]+. *Angew. Chem. Int. Ed. Edition* **2012**, *51*, 12077−12080.
(60) Banh, H.; Hornung, J.; Kratz, T.; Gemel, C.; Pöthig, A.; Gam, F.; Kahlal, S.; Saillard, J.-Y.; Fischer, R. A. Embryonic brass: pseudo two electron Cu/Zn clusters. *Chem. Sci.* **2018**, *9*, 8906−8913.
(61) Serafino, A.; Camedda, N.; Lanzi, M.; Della Ca', N.; Cera, G.; Maestri, G. Inter/Intramolecular Cascade of 1,6-Enynes Catalyzed by All-Metal Aromatic Tripalladium Complexes and Carboxylic Acids. *J. Org. Chem.* **2021**, *86*, 15433−15452.
(62) Cecchini, C.; Lanzi, M.; Cera, G.; Malacria, M.; Maestri, G. Complementary Reactivity of 1,6-Enynes with All-Metal Aromatic Trinuclear Complexes and Carboxylic Acids. *Synthesis* **2019**, *51*, 1216−1224.
(63) Li, X.; Li, J.; Wang, X.; Wu, L.; Wang, Y.; Maestri, G.; Malacria, M.; Liu, X. Photoelectric properties of aromatic triangular tri-palladium complexes and their catalytic applications in the Suzuki−Miyaura coupling reaction. *Dalton Trans.* **2021**, *50*, 11834−11842.
(64) Campos, J.; Nova, A.; Kolychev, E. L.; Aldridge, S. A Combined Experimental/Computational Study of the Mechanism of a Palladium-Catalyzed Bora-Negishi Reaction. *Chem. - Eur. J.* **2017**, *23*, 12655−12667.
(65) Yun, Y.; Sheng, H.; Yu, J.; Bao, L.; Du, Y.; Xu, F.; Yu, H.; Li, P.; Zhu, M. Boosting the Activity of Ligand-on Atomically Precise Pd3Cl Cluster Catalyst by Metal-Support Interaction from Kinetic and Thermodynamic Aspects. *Adv.Synth. Catal.* **2018**, *360*, 4731−4743.
(66) Bao, L.; Zhao, C.; Li, S.; Zhu, Y. Benzalaniline from nitrobenzene and benzaldehyde catalyzed efficiently by an atomically precise palladium nanocluster. *Chin. J. Catal.* **2019**, *40*, 1499−1504.
(67) Usui, R.; Sunada, Y. Triangular Palladium Cluster from Activation of the Si−Si Bond in a Disilane with Phosphine Pendants. *Inorg. Chem.* **2021**, *60*, 15101−15105.
(68) Shimamoto, K.; Sunada, Y. Dimensionality Expansion of a Butterfly Shaped Pd_4 Framework: Constructing Edge-Sharing Pd_6 Tetrahedra. *Chem. - Eur. J.* **2019**, *25*, 3761−3765.
(69) Suginome, M.; Oike, H.; Park, S.-S.; Ito, Y. Reactions of Si−Si σ-Bonds with Bis(t-alkyl isocyanide)palladium(0) Complexes. Synthesis and Reactions of Cyclic Bis(organosilyl)palladium Complexes. *Bull. Chem. Soc. Jpn.* **1996**, *69*, 289−299.
(70) Sunada, Y.; Haige, R.; Otsuka, K.; Kyushin, S.; Nagashima, H. A ladder polysilane as a template for folding palladium nanosheets. *Nature Comm.* **2013**, *4*, 2014.
(71) Yanagisawa, C.; Yamazoe, S.; Sunada, Y. Silylene-Bridged Tetranuclear Palladium Cluster as a Catalyst for Hydrogenation of Alkenes and Alkynes. *ChemCatChem.* **2021**, *13*, 169−173.

https://doi.org/10.1021/acscatal.2c03345
ACS Catal. 2022, 12, 11615−11638

(72) Sunada, Y.; Taniyama, N.; Shimamoto, K.; Kyushin, S.; Nagashima, H. Construction of a Planar Tetrapalladium Cluster by the Reaction of Palladium(0) Bis(isocyanide) with Cyclic Tetrasilane. *Inorganics* **2017**, *5*, 84.
(73) Chai, J.; Tian, R.; Wu, D.; Wei, D.; Xu, Q.; Duan, Z.; Mathey, F. *Dalton Trans.* **2018**, *47*, 13342−13344.
(74) Murahashi, T.; Fujimoto, M.; Oka, M.-A.; Hashimoto, Y.; Uemura, T.; Tatsumi, Y.; Nakao, Y.; Ikeda, A.; Sakaki, S.; Kurosawa, H. Discrete sandwich compounds of monolayer palladium sheets. *Science* **2006**, *313*, 1104−1107.
(75) Murahashi, T.; Hashimoto, Y.; Chiyoda, K.; Fujimoto, M.; Uemura, T.; Inoue, R.; Ogoshi, S.; Kurosawa, H. Reductive Coupling of Metal Triangles in Sandwich Complexes. *J. Am. Chem. Soc.* **2008**, *130*, 8586−8587.
(76) Lv, C.; Cheng, H.; He, W.; Shah, M. I. A.; Xu, C.; Meng, X.; Jiao, L.; Wei, S.; Li, J.; Liu, L.; Li, Y. Pd3 cluster catalysis: Compelling evidence from in operando spectroscopic, kinetic, and density functional theory studies. *Nano Res.* **2016**, *9*, 2544−2550.
(77) Ren, J.; Lan, P. C.; Chen, M.; Zhang, W.; Ma, S. Heterogenization of Trinuclear Palladium Complex into an Anionic Metal−Organic Framework through Postsynthetic Cation Exchange. *Organometallics* **2019**, *38*, 3460−3465.
(78) Fairlamb, I. J. S.; Scott, N. W. J. In *Nanoparticles in Catalysis*, Kobayashi, S., Ed.; Springer International: 2020; pp 171−205.
(79) Eremin, D. B.; Ananikov, V. P. Understanding active species in catalytic transformations: From molecular catalysis to nanoparticles, leaching, "Cocktails" of catalysts and dynamic systems. *Coord. Chem. Rev.* **2017**, *346*, 2−19.
(80) Reay, A. J.; Fairlamb, I. J. S. Catalytic C-H bond functionalisation chemistry: the case for quasi-heterogeneous catalysis. *Chem. Commun.* **2015**, *51*, 16289−16307.
(81) Zhao, Y.; Du, L.; Li, H.; Xie, W.; Chen, J. Is the Suzuki−Miyaura Cross-Coupling Reaction in the Presence of Pd Nanoparticles Heterogeneously or Homogeneously Catalyzed? An Interfacial Surface-Enhanced Raman Spectroscopy Study. *J. Phys. Chem. Lett.* **2019**, *10*, 1286−1291.
(82) Collins, G.; Schmidt, M.; McGlacken, G. P.; O'Dwyer, C.; Holmes, J. D. Stability, Oxidation, and Shape Evolution of PVP-Capped Pd Nanocrystals. *J. Phys. Chem. C* **2014**, *118*, 6522−6530.
(83) Collins, G.; Schmidt, M.; O'Dwyer, C.; Holmes, J. D.; McGlacken, G. P. The origin of shape sensitivity in palladium-catalyzed Suzuki-Miyaura cross coupling reactions. *Angew. Chem., Int. Ed.* **2014**, *53*, 4142−4145.
(84) Thathagar, M. B.; ten Elshof, J. E.; Rothenberg, G. Pd Nanoclusters in C−C Coupling Reactions: Proof of Leaching. *Angew. Chem., Int. Ed.* **2006**, *45*, 2886−2890.
(85) Sun, B.; Ning, L.; Zeng, H. C. Confirmation of Suzuki−Miyaura Cross-Coupling Reaction Mechanism through Synthetic Architecture of Nanocatalysts. *J. Am. Chem. Soc.* **2020**, *142*, 13823−13832.
(86) Tang, D. T. D.; Collins, K. D.; Ernst, J. B.; Glorius, F. Pd/C as a Catalyst for Completely Regioselective C−H Functionalization of Thiophenes under Mild Conditions. *Angew. Chem., Int. Ed.* **2014**, *53*, 1809−1813.
(87) Collins, K. D.; Honeker, R.; Vásquez-Céspedes, S.; Tang, D.-T. D.; Glorius, F. C−H arylation of triphenylene, naphthalene and related arenes using Pd/C. *Chem. Sci.* **2015**, *6*, 1816−1824.
(88) Costa, P.; Sandrin, D.; Scaiano, J. C. Real-time fluorescence imaging of a heterogeneously catalyzed Suzuki−Miyaura reaction. *Nat. Catal.* **2020**, *3*, 427−437.
(89) Reay, A. J.; Fairlamb, I. J. Catalytic C−H bond functionalisation chemistry: The case for quasi-heterogeneous catalysis. *Chem. Commun.* **2015**, *51*, 16289−16307.
(90) Tromp, M.; Sietsma, J. R. A.; van Bokhoven, J. A.; van Strijdonck, G. P. F.; van Haaren, R. J.; van der Eerden, A. M. J.; van Leeuwen, P. W. N. M.; Koningsberger, D. C. Deactivation processes of homogeneous Pd catalysts using in situ time resolved spectroscopic techniques. *Chem. Commun.* **2003**, 128−129.
(91) Appleby, K. M.; Dzotsi, E.; Scott, N. W. J.; Dexin, G.; Jeddi, N.; Whitwood, A. C.; Pridmore, N. E.; Hart, S.; Duckett, S. B.; Fairlamb, I. J. S. Bridging the Gap from Mononuclear PdII Precatalysts to Pd Nanoparticles: Identification of Intermediate Linear $[Pd_3(XPh_3)_4]^{2+}$ Clusters as Catalytic Species for Suzuki−Miyaura Couplings (X = P, As). *Organometallics* **2021**, *40*, 3560−3570.
(92) Kannan, S.; James, A. J.; Sharp, P. R. [Pd3(PPh3)4]2+, a New Palladium Triphenylphosphine Complex. *J. Am. Chem. Soc.* **1998**, *120*, 215−216.
(93) Omondi, B.; Shaw, M. L.; Holzapfel, C. W. Synthesis and crystal structures of new palladium catalysts for the hydromethoxycarbonylation of alkenes. *J. Organomet. Chem.* **2011**, *696*, 3091−3096.
(94) Sherwood, J.; Clark, J. H.; Fairlamb, I. J. S.; Slattery, J. M. Solvent effects in palladium catalyzed cross-coupling reactions. *Green Chem.* **2019**, *21*, 2164−2213.
(95) Hyotanishi, M.; Isomura, Y.; Yamamoto, H.; Kawasaki, H.; Obora, Y. Surfactant-free Synthesis of Palladium Nanoclusters for Their Use in Catalytic Cross-coupling Reactions. *Chem. Commun.* **2011**, *47*, 5750−5752.
(96) Ishida, J.; Nakatsuji, M.; Nagata, T.; Kawasaki, H.; Suzuki, T.; Obora, Y. Synthesis and Characterization of N,N-Dimethylformamide-Protected Palladium Nanoparticles and their use in the Suzuki-Miyaura Cross-Coupling Reaction. *ACS Omega* **2020**, *5*, 9598−9604.
(97) Zhang, L.; Li, Z.; Zhang, Y.; Paau, M. C.; Hu, Q.; Gong, X.; Shuang, S.; Dong, C.; Peng, X.; Choi, M. M. F. High-performance Liquid Chromatography Coupled with Mass Spectrometry for Analysis of Ultrasmall Palladium Nanoparticles. *Talanta* **2015**, *131*, 632−639.
(98) Adrio, L. A.; Nguyen, B. N.; Guilera, G.; Livingston, A. G.; Hii, K. K. Speciation of Pd(OAc)2 in ligandless Suzuki−Miyaura reactions. *Catal. Sci. Technol.* **2012**, *2*, 316−323.
(99) Bedford, R. B.; Bowen, J. G.; Davidson, R. B.; Haddow, M. F.; Seymour-Julen, A. E.; Sparkes, H. A.; Webster, R. L. Facile Hydrolysis and Alcoholysis of Palladium Acetate. *Angew. Chem., Int. Ed.* **2015**, *54*, 6591−6594.
(100) Rosner, T.; Le Bars, J.; Pfaltz, A.; Blackmond, D. G. Kinetic Studies of Heck Coupling Reactions Using Palladacycle Catalysts: Experimental and Kinetic Modeling of the Role of Dimer Species. *J. Am. Chem. Soc.* **2001**, *123*, 1848−1855.
(101) Amatore, C.; Jutand, A.; Le Duc, G. Mechanistic Origin of Antagonist Effects of Usual Anionic Bases (OH−, CO32−) as Modulated by their Countercations (Na^+, Cs^+, K^+) in Palladium-Catalyzed Suzuki−Miyaura Reactions. *Chem. - Eur. J.* **2012**, *18*, 6616−6625.
(102) Amatore, C.; Jutand, A.; Le Duc, G. The Triple Role of Fluoride Ions in Palladium-Catalyzed Suzuki−Miyaura Reactions: Unprecedented Transmetalation from $[ArPdF(L)_2]$ Complexes. *Angew. Chem., Int. Ed.* **2012**, *51*, 1379−1382.
(103) Hartwig, J. F. *Organotransition metal chemistry: from bonding to catalysis*; University Science Books: 2010.
(104) Cartwright, S. J.; Dixon, K. R.; Rattray, A. D. Studies of trinuclear palladium clusters by phosphorus-31 NMR spectroscopy: reactivity of $[Pd_3Cl(PPh_2)_2(PR_3)_3][BF_4]$ complexes (R = ethyl or phenyl) and the synthesis of $[Pd_3(PPh_2)_3(PR_3)_3][BF_4]$. *Inorg. Chem.* **1980**, *19*, 1120−1124.
(105) Xu, C.-Q.; Xing, D.-H.; Xiao, H.; Li, J. Manipulating stabilities and catalytic properties of trinuclear metal clusters through tuning the chemical bonding: H_2 adsorption and activation. *J. Phys. Chem. C* **2017**, *121*, 10992−11001.

https://doi.org/10.1021/acscatal.2c03345
ACS Catal. 2022, 12, 11615−11638